Influence of inherited basement structures to the development of a sedimentary basin:
The Ombilin Basin, Sumatra, Indonesia

Master Thesis Report

Wishnu Triananda Santoso

6206492

Supervisors:

Prof. dr. Jan-Diederik van Wees

Dr. Jeroen Smit

Lukman Sutrisno, M.Si

Universiteit Utrecht

Department of Earth Science

Utrecht University

July 2020

Abstract

The Ombilin Basin is one of several Tertiary basins that are presently located in the Sumatran Arc, in close vicinity of the active dextral strike-slip Sumatran Fault System (SFS) and surrounded by an active Quaternary volcanic complex. The Cenozoic geologic history of the basin is subjected to the oblique convergence between the Indo-Australian oceanic plate to the southwestern edge of Sundaland. The Ombilin Basin formed in the Paleogene and as its origin pre-dates the Mid-Miocene SFS, its basin architecture, therefore, forms an excellent recorder of tectonism in the pre- and early history of the SFS. Since the early Paleogene strata are well exposed in this basin, the Ombilin Basin can be considered as an analogue for other Sumatran basins, especially their syn-rift phase. Using surface geology, detailed Digital Elevation Models (DEM), and subsurface data i.e., 2D seismic lines and exploration wells, the study has been conducted to decipher the initial condition, development, and current interior structures of the basin in response to the regional tectonic settings. The research reveals that the Ombilin Basin originated in the extensional phase of Sumatra since the Early Paleogene to the Early Miocene. The geometry and structural development of the basin was then controlled by the NW-SE inherited structural fabrics, which later inverted since the Mid-Miocene onward during the intensive growth of the Barisan Orogeny. A new model for the basin development is then proposed.

Keywords: Tectonic, basin origin, geological modeling, seismic interpretation, Ombilin Basin, Sumatra, Indonesia

Table of Contents

Abstract 1
Table of Contents 2
List of Figures 3
1. Introduction 7
2. Geological Background 8
2.1. Tectonic Setting 8
2.1.1. Pre-Tertiary Tectonic 9
2.1.2. Tertiary Tectonic and Stratigraphic evolution 11
3. Data and Methodology 14
3.1. Digital Elevation Model (DEM) 14
3.2. Seismic data 15
3.3. Well data 15
3.4. Seismic interpretation 16
3.5. Time-to-depth conversion 16
4. Result 17
4.1. The surface structural trends of the Ombilin Basin 17
4.1.1. The Lineaments at the Ombilin Basin in comparison with the geology 18
4.2. Basin geometry 20
4.3. Ombilin Basin structure 21
4.4. Seismic interpretation of the Sinamar Sub-basin 21
4.5. The Interior Structure of the Sinamar Sub-basin 23
4.6. The depth structure maps 28
5. Discussion 30
5.1. Rifting model of the Ombilin Basin 30
5.2. Comparison to other Tertiary basins in Sumatra 34
6. Conclusion 37
7. Recommendation for further studies 38
Acknowledgment 39
References 40
Appendix 43

List of Figures

Figure 1. Map showing Sumatra Island with the location of the research area. The Ombilin Basin inside the yellow box in comparison with other basins, which are indicated by the orange dashed line (North Sumatra, Central Sumatra, and South Sumatra basin). 7

Figure 2. Regional structural setting of Sumatra including the Ombilin Basin. Right: The subsurface structures after (Barber et al., 2005) and (Heidrick & Aulia, 1993) with the Ombilin Basin (green line) and other basins including Central Sumatra basin (dashed line). Left: The regional cross-section after Koning (1985). 8

Figure 3. Pre-Tertiary tectonic evolution of the Sundaland. (Redrawn from Barber et al. (2005), positions of the SW. Borneo and Woyla blocks from Hall (2012)). 10

Figure 4. A) Tectonic block configuration of Sumatra by Late Cretaceous (around 90 Ma) which from the west to the east comprised of the Woyla Arc, West Sumatra Block, and Sibumasu Block respectively (Redrawn from Barber et al. (2005)). B & C: the Schematic cross-section of the southwestern margin of Sundaland in the Middle to Late Cretaceous respectively (Redrawn from Barber et al. (2005) in Advokaat et al., (2018)). 11

Figure 5. The tectonic evolution of SE Asia by showing the nature of the basin fill together with the rifting timing from Eocene to the Late Miocene (Hall & Morley, 2004)..... 12

Figure 6. Stratigraphy of the Ombilin Basin after Habrianta et al., (2018) and Koesoemadinata & Matasak (1981), including the regional tectonostratigraphic event after Barber et al. (2005) 13

Figure 7. The availability of two-dimensional seismic lines at the Ombilin Basin. The seismic lines mostly cover the Sinamar Sub-basin. The total length of good-interpretable seismic lines is 733,871.94 meters (blue lines) while the length of the poor-quality seismic line is 140,372.75 meters (red lines). 15

Figure 8. The linear function of seismic time versus depth of each interpreted stratigraphic unit. A total of six wells were utilized to produce the linear function. The graphs show a good spatial distribution of time versus depth on each stratigraphic unit. The depth conversion was applied by simply multiplying the function to each time-domain surface. 17

Figure 9. The structural trend of the Ombilin Basin from the lineament extraction of the Digital Elevation Model (DEM) using multi-directional hill shades: from azimuth 45˚, 135˚, 225˚, 315˚. The Ombilin Basin is dominated by the NW-SE trend (red line) and N-S (yellow line), also some other minor trends, such as the E-W (pink line), and the NE-SW (green line). 18

Figure 10. The NW-SE trend in the research area in comparison with the lineament of basement fabrics from the gravity data interpretation (after Sutrisno et al., in prep). The N-S trend looks like a series of NS fault structures. 19

Figure 11. Regional Geological map of the Ombilin Basin overlying the topographic map of the Digital Elevation Model (DEM) modified from Silitonga & Kastowo (1975), Koning (1985), and Situmorang et al. (1991). The fault lines were updated using the interpretation of the Digital Elevation Model and the seismic survey that was used in this study. The older strata of Paleocene- Eocene Brani and Sangkarewang formations represented by brown and dark green, respectively, are mainly exposed in the Talawi area while only some position of Sangkarewang Formation exposed in the southern part of Sinamar area. From this map, we can determine that different rates of erosion affected the Ombilin Basin. 20

Figure 12. The Inline seismic section (section AA') of the Sinamar Sub-basin shows the interpretation of seismic reflection termination and overview of seismic facies. In general, several features can be identified such as the unconformity from the truncation of the reflectors (yellow box), the possible alluvial-fan or fan-delta deposit in the middle part of the section (green box) and the reflection configuration as well as the continuity of the reflectors (blue box). Location see Figure 11. 22

Figure 13. The crossline seismic section (section DD') of the Sinamar Sub-basin shows the interpretation of seismic reflection termination and overview of seismic facies. In general, several features can be identified such as the chaotic seismic facies (red box), the possible slope channel within Brani Formation (blue box) the multi-story of the braided river system (green box), and the interface of Sawahtambang Formation by amplitude contrast (yellow box). Location see Figure 11. 22

Figure 14. The arbitrary seismic section in NW-SE orientation (section FF') of the Sinamar Sub-basin shows the identification of each top formation using wireline logs by Habrianta et al. (2018). The yellow and green color fill in the wireline logs represents the sand and shale dominated lithology, respectively. Location see Figure 11 23

Figure 15. The Inline seismic section (section AA') of the Sinamar Sub-basin. The thickest sediment or the deepest basin center is recorded in this seismic section. The sediments are wedding to the northwest direction. The deepest well of Sinamar-1 (S1) is crossed by this inline section. Location see Figure 11. 24

Figure 16. A) The flatten horizon at the top of the Paleocene-Early Eocene Sangkarewang Fm. (the early syn-rift phase). B) The flatten horizon at the top of the Oligocene Sawahtambang Fm (the late syn-rift phase). The deepening of the half-graben was controlled by the fault L6 on the NW side that acted as the master fault. 24

Figure 17. The seismic cross section of SW-NE direction (section BB') is in the North Limb area. The normal fault on the southwest is the Sitangkai Fault. The surface and subsurface deformation is less likely affecting the area instead of this place is the narrowest area of the Sinamar Sub-basin. Only several folding structures exist, and the sediments are gently dipping to the northwest. VE is vertical exaggeration. Location see Figure 11. The fault L3 in this section is the component of Takung Fault of which portion of the Sawahtambang Formation (Oligocene) is thrust over the younger basin fill..... 25

Figure 18. The crossline seismic section (section CC') of the Sinamar Sub-basin. The fault L1 and L2 are the NW-SE inherited basement fabrics. The Tanjung Ampalo Fault is the N-S oriented structure as the master fault during the rifting phase, which later reactivated as dextral strike-slip during basin inversion in Mid-Miocene and the development of back-thrusting. The anastomosing fault pattern that is found from the surface interpretation created a positive flower structure during the basin inversion. Location see Figure 11. 26

Figure 19. The crossline seismic section (section DD') of the Sinamar Sub-basin. The fault L1, L2, and L3 are the NW-SE inherited basement fabrics that reactivated as reverse fault during the basin inversion (Mid-Miocene). The Tanjung Ampalo Fault is the N-S oriented structure as the master fault during the rifting phase, which later reactivated as dextral strike-slip during basin inversion in Mid-Miocene and the development of back-thrusting. The anastomosing fault pattern that is found from the surface interpretation created a positive flower structure during the basin inversion. Location see Figure 11. 26

Figure 20. The crossline seismic section (section EE') located in the southeast of the Sinamar Sub-basin. The fault L4 is the NW-SE inherited basement fabrics. Little deformation affecting the area due to its location in the basin edge. The fault L4 reactivated as reverse fault during the inversion (Mid-Miocene)

creating Palangki Anticline where some portion of the Oligocene Sawahtambang Formation is exposed. The anastomosing fault pattern that is found from the surface interpretation created a positive flower structure during the basin inversion. Location see Figure 11. 27

Figure 21. The depth structure map of Top Pre-Tertiary Basement that has been combined with the basement outcrop (orange to red color) from the surface geology map. The basement is dominated by the N-S and NW-SE trend structure. The deepest depocenter is near the Guguk area on the south of Takung Fault. 28

Figure 22. The depth structure map of Top Brani Formation. The structure is dominated by the N-S and NW-SE trend faults. The deepest depocenter is near the Guguk area on the south of Takung Fault. 29

Figure 23. The depth structure of Top Sangkarewang Formation. The structure is dominated by the N-S and NW-SE trend faults. The deepest depocenter is near the Guguk area on the south of Takung Fault. 29

Figure 24. The depth structure of Top Sawahtambang Formation that has been combined with the outcrop data (the area inside the dashed line) from the surface geology map. The structure is dominated by the NW-SE trend faults. Because the rifting started to stop at the end of Sawahtambang Formation, the N-S structure is barely seen in this map. The deepest depocenter is near the Guguk area on the south of Takung Fault. 30

Figure 25. The thickness map of the early rift units and the rifting mechanism. The early syn-rift of the Ombilin Basin in the Paleocene-Early Eocene and the deposition of Brani Formation (Tob) interfingers with Sangkarewang Formation (Tos) during the early Paleogene extension. The rifting was accommodated by the N-S trend structure (red line) that acted as the master fault and the NW-SE trend inherited basement fabrics (pink line) as transfer fault creating the N-S oriented. The thickest sediment and deepest depocenter of the Sinamar Sub-basin are located in the northern center area. This is due to the segmented rifting mechanism in the Ombilin Basin. 31

Figure 26. The thickness map of the late syn-rift units (the Late Eocene Sawahlunto Formation and the Oligocene Sawahtambang Formation (both represented by Tmol)). A similar rifting mechanism model still affecting the development of the basin in the Late Eocene-Late Oligocene. This phase is marked by the erosion of the early sin-rift units in the SE area of the basin edge while the deposition of the late syn-rift units. 31

Figure 27. The total thickness of the syn-rift sediments. The thickest sediment around 4500 m in the northern center area has been deposited from the Early Cenozoic to the Late Oligocene. 32

Figure 28. The present-day thickness map of the Early Miocene Ombilin Formation (Tmou). The thickest preserved post-rift unit is deposited in the North Limb area (ca. 1500 m thick). The preserved thickness of the Ombilin formation that is thinner in the SE area is subjected to the extensive erosion following the basin inversion since the Mid-Miocene. 32

Figure 29. The basin inversion that occurred in the Mid-Miocene yield the rejuvenation of the early N-S fault and the NW-SE inherited basement fabrics to become the reverse faulting and some of the N-S faults became strike-slip faults. This is together with the development of the back-thrusting as a conjugate fault and the NW- SE trend folds, which can be seen from the NE-SW seismic profile (Figure 18, Figure 19, Figure 20). Continuous compressional setting in the Plio-Pleistocene tectonic phase induced the development of several strike-slip faults, including the NW-SE anastomosing fault pattern and the NE-SW sinistral strike-slip. 33

Figure 30. The model development of the Bengkalis graben by Moulds (1989). 34

Figure 31. The Moulds (1989) model on the Ombilin Basin. The N-S oriented faults that are bounded by the NW-SE inherited basement fabrics acted as the master fault when the rifting occurred, and the side grabens developed as a result of continuous segmented rifting..... 35

Figure 32. The figure showing the present geometry and trend of the basin depocenters in Sumatra (modified from Pubellier & Morley, 2014) with the inset of North Sumatra Basin (cyan box) from Barber et al. (2005), the Central Sumatra Basin (red box) from Heidrick & Aulia (1993), and the South Sumatra Basin (blue box) from Ginger & Fielding (2005)..... 35

Figure 33. Map to show the position of Ninety East Ridge (modified from Hall, 2012)..... 36

Figure 34. (A) Oroclinal bending model of Hutchison (1994) in Hutchison (2014). The regional solid lines are the strike lines of Triassic strata. (B) The inset to show the anticlockwise rotation of Borneo by Advokaat, Marshall, et al. (2018). (C) The inset to show the clockwise rotation of Thai-Malay Peninsular as an implication of IndoChina rotation by (Li et al., 2017)..... 37

1. Introduction

The Ombilin Basin is one of several basins in Sumatra, Indonesia. It lies along the strike-slip deformation zone of a large dextral fault system, the Sumatran Fault System (SFS) (Figure 1). Formed in the Paleogene, the Ombilin pre-dates the Miocene Sumatran Fault System and may thus provide information on the pre- and early history of the Sumatran Fault System.

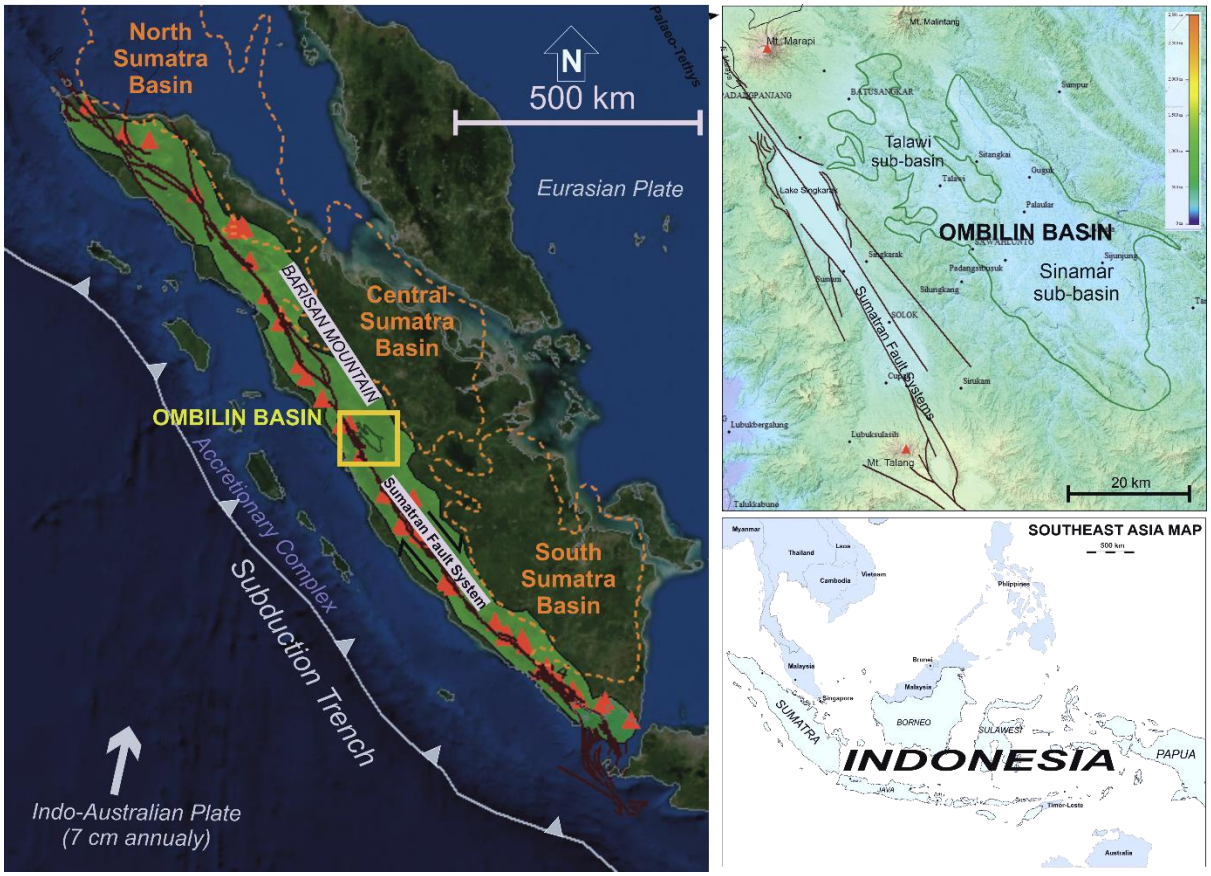

Figure 1. Map showing Sumatra Island with the location of the research area. The Ombilin Basin inside the yellow box in comparison with other basins, which are indicated by the orange dashed line (North Sumatra, Central Sumatra, and South Sumatra basin).

The Ombilin Basin is situated just next to the Sumatran Arc where the dextral Sumatran Fault coexists with the Quaternary volcanic centers. The Ombilin Basin extends in the NW-SE direction with sub-rhombohedral geometry around 1500 km^2. The orientation of the Ombilin Basin is at an angle of approximately 20 degrees with respect to the Sumatran Fault System. The basin consists of two main depocenters, the Talawi and a larger one, the Sinamar. The Talawi sub-basin is in the northwest of the basin and has been up-thrown and heavily eroded, resulting in exposure of lower-lying Tertiary strata. The Sinamar sub-basin is the down-thrown part that extends from the northeast of the Talawi sub-basin divided by the basement high of Pre-Tertiary rock at Bukit Tungkar (Koesoemadinata & Matasak, 1981) and the N-S structural trend to the entire southern area.

The Ombilin Basin is located on the southwest side of the Central Sumatra Basin, which is a much larger basin (Figure 2). According to Barber et al. (2005), the horst and graben stage in the Late Eocene-Oligocene developed a mountainous landscape with an isolated lake in the region of the Ombilin Basin. In a later stage, during the initiation of Barisan Orogeny in the Late Miocene, Barber et al. (2005) suggested that the Ombilin was separated from the rest of the Central Sumatra Basin (Barber et al., 2005). Subsequently, located at the eastern edge of the Barisan Orogenic belt, Ombilin Basin

experienced uplifting and erosion which removed most of the Ombilin Neogene strata. At present day, it is considered an intra-montane basin, which is surrounded by a Quaternary volcanic complex (Barber et al., 2005).

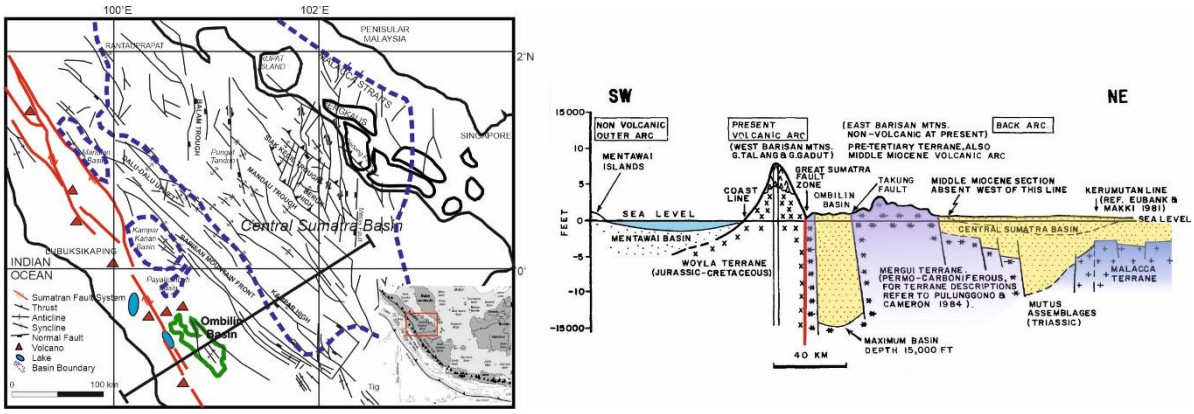

Figure 2. Regional structural setting of Sumatra including the Ombilin Basin. Right: The subsurface structures after (Barber et al., 2005) *and* (Heidrick & Aulia, 1993) *with the Ombilin Basin (green line) and other basins including Central Sumatra basin (dashed line). Left: The regional cross-section after* Koning (1985).

However, the development of the Ombilin Basin seems more complicated, reflected in contradicting concepts regarding the origin of the basin. Koesoemadinata & Matasak (1981) suggested that the development of the Ombilin Basin began with the formation of a graben-like depression that resulted from block faulting following the tensional stresses of Upper Cretaceous orogenesis. This graben-like depression was filled by the Tertiary lake deposits to transgressive marine sediments at the end of its deposition cycle. Alternatively, Koning (1985) suggested that the Ombilin Basin is a graben-like, pull apart structure that formed as a product of the Early Tertiary tensional tectonics of the Great Sumatran Fault Zone. Then, Situmorang et al. (1991) postulated that the dextral motion of the Sumatran Fault System controlled the structural development of the Ombilin Basin. Later on, those arguments were contested by Howells (1997) interpreting the Ombilin Basin not as a pull-apart basin but rather a more complex story of wrench-modified rift basin. He argued its genetic origin was similar to the other early Tertiary basins of Sumatra, which originated by normal fault displacements. Noeradi et al., (2005) also considered the Ombilin Basin as a rift-related basin.

Therefore, this study was conducted to reconstruct the geometry of the Ombilin Basin and its structural features that have been developed in response to the occurrence of regional tectonic settings. The newly drilled exploration wells together with the seismic lines and detailed Digital Elevation Model were used in order to decipher its structural development. Hence, a new model for the origin of the Ombilin Basin is proposed.

2. Geological Background

Reconstructing the geometry and the structural elements of the basin requires an understanding of its regional geology. Therefore, the tectonic evolution of the Sumatra as a whole and the Ombillin Basin including its associated stratigraphic units are described in this section.

2.1. Tectonic Setting

Sumatra is the biggest island in the western Indonesian archipelago. The current structure of Sumatra is mainly affected by the northward subduction of the Indian Plate under the Eurasian Plate at an approximate rate of 7 cm a^{-1}. The subduction is oblique relative to the island's NW-SW orientation. The convergent movement of these plates yields the main structural features and the development of several Tertiary basins in Sumatra, which is divided into three regions (Barber et al., 2005): the

forearc, the Barisan Mountains including the Sumatran Fault System and volcanic chain, and the backarc region.

The Barisan Mountains concurrently extend along the whole length of Sumatra and include the uplifted Pre- Tertiary rocks of Permo-Carboniferous to Cretaceous age forming the basement rocks of Sumatra, and which are overlain by the Tertiary sediments and volcanics as well as the recent volcanic products (Barber et al., 2005).

Sumatra as a whole is part of a bigger tectonic block, Sundaland, which has been developed since the Devonian (Barber et al., 2005). Since the basin is composed of the Pre-Tertiary basement and the Tertiary basin fill, hence, the tectonic outline is narrated in two sections: Pre-Tertiary and Tertiary.

2.1.1. Pre-Tertiary Tectonic

Sundaland was formed by several accreted Gondwana-derived crustal blocks (continental and oceanic microplates) of Indochina/East Malaya, which include the Cathaysia, Sibumasu, and West Sumatra blocks. These blocks were detached from Gondwana initiated by the opening of the Palaeo-Tethys (Figure 3A) that separated the Indochina/East Malaya and the West Sumatra Block from the northeastern margin of the Gondwana in the Devonian (Metcalfe, 2013; Barber et al., 2005).

During the Carboniferous to the Early Permian (Figure 3B), the northward rifting of the Sibumasu from Gondwana, with the West Sumatra Block forming its southern continental margin, resulted in the development of the Meso-Tethys (Barber et al., 2005). The Permo-Carboniferous metasediments of the Kuantan Formation are suggested as a continental margin sediment product of the West Sumatra Block (Barber et al., 2005). The Kuantan Formation is composed of lower grade metamorphic rocks: quartzite, phyllite/slate, and recrystallized limestone. In the present-day, this formation can be found extensively exposed on the east to the south of the Ombilin Basin.

Later in the Mid-Permian, rifting of the Meso-Tethys ocean evoked the detachment of the West Sumatra Block from northern Gondwana (Figure 3B). Meanwhile in the northern area, the northward subduction of Sibumasu beneath the East Malaya closing the Palaeo-Tethys and generated an Andean-type magmatic arc in the West Sumatra Block. In the Ombilin Basin, the product of this tectonic event is the Silungkang Formation of Mid-Permian age (Barber et al., 2005), composed of volcanic materials, andesite, basaltic lava, tuff, and limestone. The formation can be found around the Silungkang Village between the Sawahlunto and the Solok area (Silitonga & Kastowo, 1975; Koesoemadinata & Matasak, 1981; Barber et al., 2005).

The collision of Sibumasu with East Malaya in the Late Permian (Figure 3C) created the accretionary complex of the Malay Peninsula, the Bentong-Raub Suture Zone (Barber et al., 2005; Metcalfe, 2013; Advokaat et al., 2018). During this time, the Permo-Triassic sediments of the Tuhur Formation were deposited, which is composed of re-crystalline limestone, slate, and shale (Silitonga & Kastowo, 1975; Barber et al., 2005). In the present-day, this formation is sparsely outcropped on the east of Lake Singkarak and the southwest of the Ombilin Basin.

In the Early Triassic, the continuous expansion of the Meso-Tethys ocean provoked the translation of the West Sumatra Block from the southeast of East Malaya to its present position, on the west of Sibumasu (Figure 3D) (Barber et al., 2005). This major NW-SE transcurrent strike-slip, which is now recognized as the Medial Sumatra Tectonic Zone (MSTZ) (Figure 3D) (Barber et al., 2005; Metcalfe, 2013). The transcurrent movement was inferred since there are no former ocean basin rocks or ophiolitic remnants found within the MSTZ that would represent a true suture (Metcalfe, 2013). These three major blocks, the East Malaya, the Sibumasu, and the West Sumatra Block together form Sundaland.

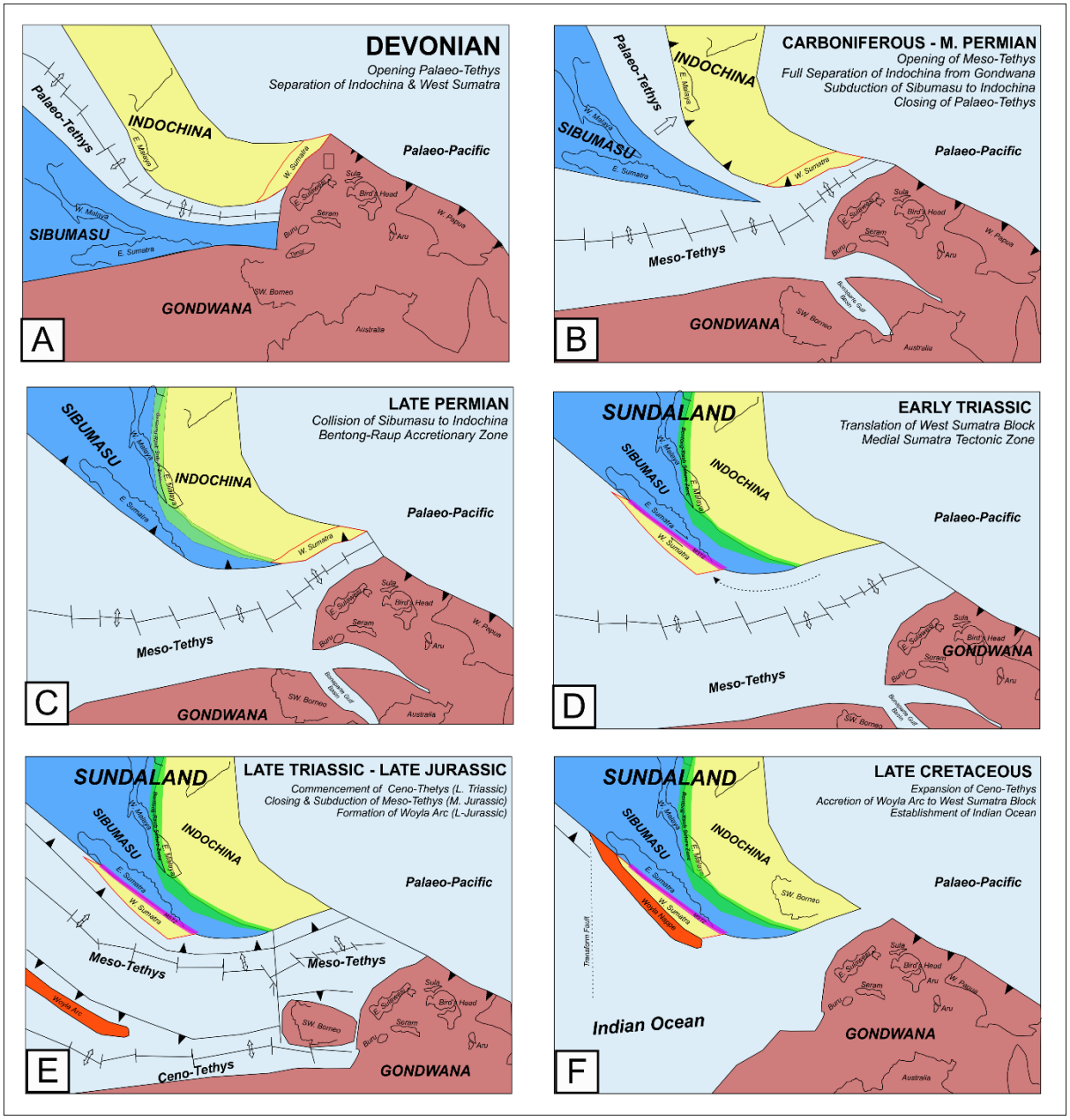

Figure 3. Pre-Tertiary tectonic evolution of the Sundaland. (Redrawn from Barber et al. (2005), positions of the SW. Borneo and Woyla blocks from Hall (2012)).

Through the Mid- and Late Triassic, the NE-SW regional extension phase occurred in the whole of Sumatra and Peninsular Malaya. This resulted in the development of several north-south and NW-SE trending horsts and grabens. In Sumatra, these include the Kualu and Tuhur basins and the Medial Sumatra High (Barber et al., 2005). Carbonates were deposited on the horst blocks while the terrigenous sediments of cherts in the grabens suggest sediment-starved conditions (Barber et al., 2005). Meanwhile, during the Late Triassic, the opening of a new ocean, the Ceno-Tethys, had commenced on the south of Meso-Tethys (Figure 3E) (Metcalfe, 2013).

Following the transcurrent motion of the West Sumatra Block in the Early Triassic, part of the Meso-Tethys Ocean segment shifted to the western coast of Sundaland (Barber et al., 2005). In the Mid-Jurassic, this segment of Meso-Tethys Ocean subducted eastward under the West Sumatra Block resulting in the Andean magmatic arc in the western part of Sibumasu (Figure 3E) (Barber et al., 2005; Metcalfe, 2013). In the present-day, this Andean arc is located in the central Sumatra (Figure 4B)

(Barber et al., 2005). The subduction also commenced westward in the late Jurassic, together with the expansion of the new ocean on the northern Gondwana, the Ceno-Tethys (Figure 3E). Subsequently, the intra-oceanic arc was formed at the southern edge of the Meso-Tethys: the Woyla Arc (Figure 3E) (Barber et al., 2005; Hall, 2012).

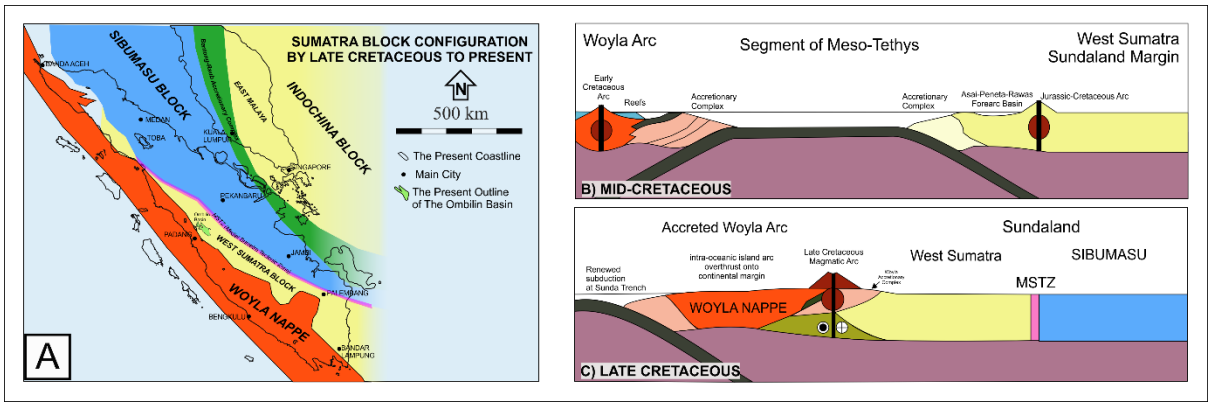

Figure 4. A) Tectonic block configuration of Sumatra by Late Cretaceous (around 90 Ma) which from the west to the east comprised of the Woyla Arc, West Sumatra Block, and Sibumasu Block respectively (Redrawn from Barber et al. (2005)*). B & C: the Schematic cross-section of the southwestern margin of Sundaland in the Middle to Late Cretaceous respectively (Redrawn from* Barber et al. (2005) *in* Advokaat et al., (2018)*).*

The widening of the Ceno-Tethys Ocean in the early Late Cretaceous led the northwards movement of the Woyla Arc towards the West Sumatra Block and the closure of the Meso-Tethys (Figure 3F) (Barber et al., 2005; Hall, 2012). Subsequently, in the early Late Cretaceous (ca. 110 Ma in the Hall (2012) model) Woyla Arc and its associated accretionary complex (oceanic assemblage) collided over the West Sumatra Block to develop the Woyla Nappe (Figure 3F) (Barber et al., 2005). Barber et al. (2005) also suggested that the collision of the Woyla Arc responsible for folding and the slaty cleavage development in pelitic rocks of Kuantan Formation. Following the collision of the Woyla Arc, the initiation of the present-day subduction of the Indo-Australian ocean plate (Indian ocean plate) beneath Sundaland evoked the initiation of the Late Cretaceous magmatic arc of the future Barisan Mountain (Figure 4C) (Barber et al., 2005).

2.1.2. Tertiary Tectonic and Stratigraphic evolution

Following the collision of the Woyla Nappe in the Late Cretaceous, Sundaland appears to have been almost completely elevated to the subaerial conditions and surrounded by passive margins (Hall, 2012). At that time, Sumatra was comprised of three tectonic blocks from west to east, the Woyla, West Sumatra, and the Sibumasu blocks, respectively (Figure 4A). Hall (2009) suggested that a passive margin was established after the termination of subduction beneath Sundaland from the early Late Cretaceous (ca. 90 Ma) until Mid-Eocene (ca. 45 Ma), as evidenced by the absence of a volcanic and plutonic record in most of Sumatra and Java. As a result, the Tertiary sediments unconformably cover the uplifted Pre-Tertiary rocks that act as a basement rock (Barber et al., 2005). Hall (2012) also suggested that moderate extension and dextral strike-slip motion may have occurred at the Sumatra and Java margin (70-65 Ma).

Consequently, the Late Cretaceous to Mid-Eocene (90-45 Ma) is marked by a period of erosion, non-deposition, and redeposition of sediments from previous volcanic activity (Hall, 2012). The Paleocene to Eocene is referred to as Pre-Rift in Sumatra.

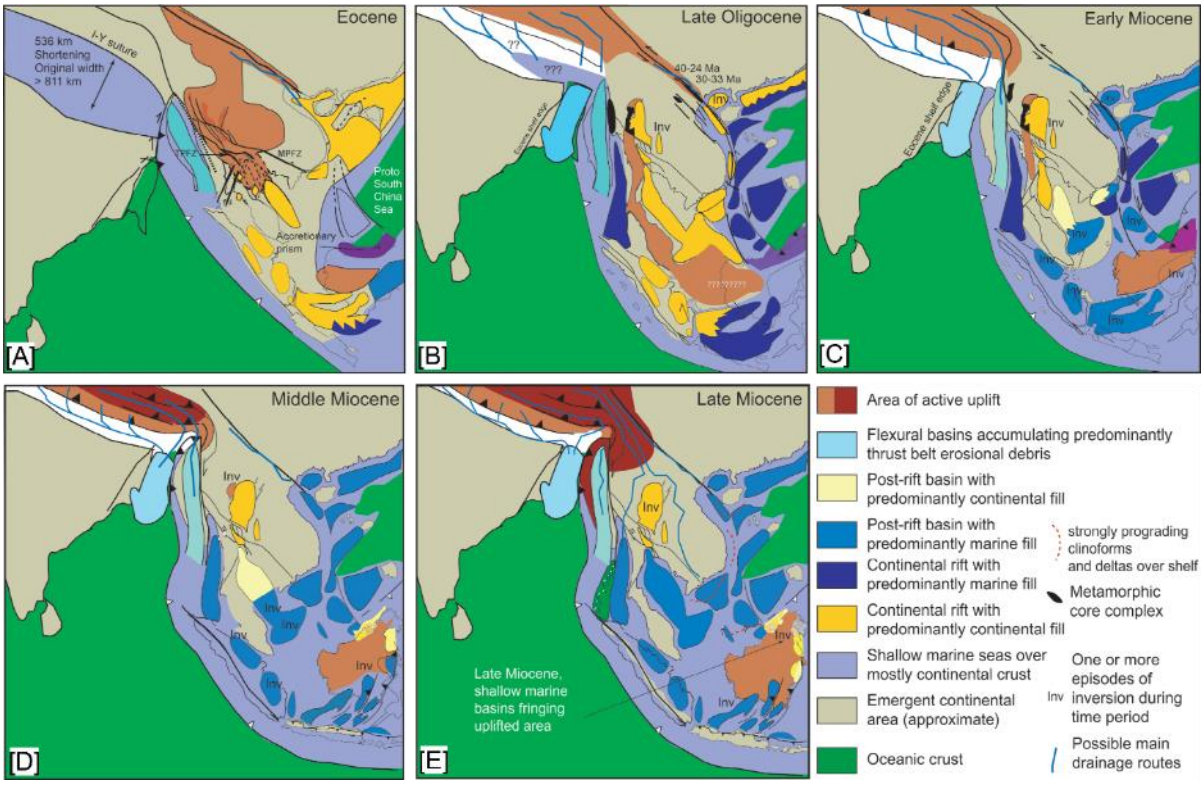

Figure 5. The tectonic evolution of SE Asia by showing the nature of the basin fill together with the rifting timing from Eocene to the Late Miocene (Hall & Morley, 2004)

The oblique subduction beneath Sumatra began in the Middle Eocene (c. 45 Ma) when the Australian plate began to move north resulting in the activation of the Sumatra-Java Arc and the development of sedimentary basins in Sundaland (Hall, 2012). In the Late Eocene to Early Oligocene, the continuous northward movement of Australia induced a regional extension forming horsts and grabens throughout Sundaland establishing a mountainous landscape (Barber et al., 2005). This Paleogene movement of Australia also evoked the development of isolated deep lacustrine basins amid the Pre-Tertiary rocks, such as the Ombilin Basin (Barber et al., 2005). The sediments that filled these basins, which characterized by the continental sediment fill, are sourced from the adjacent local horst blocks (Figure 5A) (Barber et al., 2005; Hall & Morley, 2004). In the Ombilin Basin, these are the alluvial fan of Brani Formation and lacustrine organic-rich shales of the Sangkarewang Formation that were unconformably deposited over the meta-volcanic and meta-sediments of the Pre-Tertiary basement (Barber et al., 2005).

In the same time, the development of the South China Sea in ca. the latest Eocene-Early Oligocene (Figure 5A) (Hall, 2012) evoked the regression phase in Sumatra (Husein et al., 2018). In the Ombilin Basin, the regression phase that developed in the marginal marine setting resulted in the deposition of fluvio-deltaic sediment that contains coal and the interconnected fluvial system products (Husein et al., 2018). These sediments are represented by the brown shales with coal seams of the Sawahlunto Formation and the sandstones of Sawahtambang Formation, respectively.

The age of the sediments in the horst and graben stage is not well constrained because of their terrestrial origin. However, the palynology analysis suggests the age of Sawahlunto Formation is Eocene and the Sawahtambang Formation is Oligocene (Koesoemadinata & Matasak, 1981).

Following the horst and graben stage, in the Late Oligocene, the initiation of the Barisan Mountains had commenced by the inversion of the previous graben systems leading to folding and thrusting of

syn-rift sediments (Barber et al., 2005). This was accompanied by erosion that yields to the unconformity and sediment recycled in Sumatra (Barber et al., 2005).

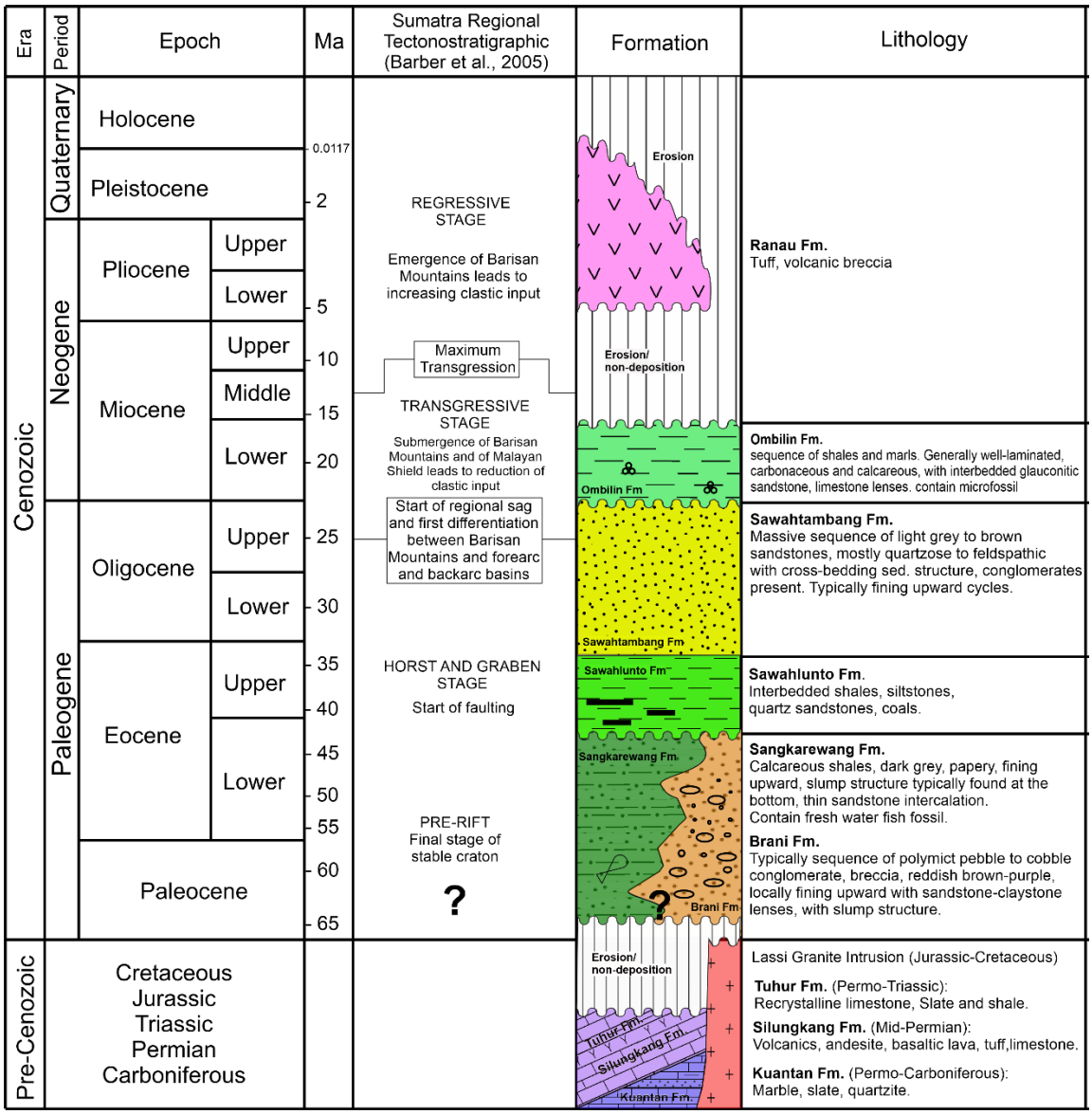

Figure 6. Stratigraphy of the Ombilin Basin after Habrianta et al., (2018) and Koesoemadinata & Matasak (1981), *including the regional tectonostratigraphic event* after Barber et al. (2005)

The uplifting phase in the Late Oligocene was followed by the regional sag and the transgressive phase in much of Sundaland including Sumatra until the Mid-Miocene. This occurred together with the recommence of the Sumatran arc system contrasting the Barisan Range with other areas (Barber et al., 2005). Subsequently, the Barisan Mountain became one of the major sediment sources for the present forearc and backarc basins area (Barber et al., 2005). This phase occurred (Barber et al., 2005).

The continuous subsidence outpaced the uplift of the early Barisan Mountains, leading to marine transgression and deposition of marine sediments in the Early Miocene (Barber et al., 2005). In the Ombilin Basin, the event was marked by the deposition of open marine shales with local reef limestone of the Ombilin Formation (Barber et al., 2005).

From the Mid-Miocene, the rapid growth of Barisan Mountain and the forearc island due to subduction of the Indian Ocean plate outpaced the regional sag during the regression phase whilst

further subsidence in the back-arc as well as forearc basins continued. The uplifting was accompanied by intense volcanism while the Barisan Mountains experienced erosion and became the major sediment source of Sumatra (Barber et al., 2005). The establishment of the dextral Sumatran Fault System also occurred during this period, at least since the Mid-Miocene (ca. 14 Ma) (Barber et al., 2005). These events coexist by the basin inversion during the Miocene, which later continued through the Plio-Pleistocene that rejuvenated the early faults (Barber et al., 2005). The Ranau Formation in the Ombilin Basin consist of volcanic products of the Late Miocene-Pliocene volcanic episode (Barber et al., 2005)

The convergence of the oblique subduction of the Indo-Australian ocean plate (Indian ocean plate) to the SW Sundaland together with the dextral transcurrent movement of the Sumatra Fault System from the early Paleogene to the present day is responsible for the structural development of the Ombilin Basin.

3. Data and Methodology

The structural features and the tectonic footprints were studied at the surface using the Digital Elevation Model while in the subsurface 2D Seismic lines and well data were used. The interpretation of the surface structures allows for the first recognition of basin structures and linking the basin to the surrounding geology. The basin structure and tectonic development, including the syn-sedimentary deposits, were then studied in cross-section using a grid of 2D seismic lines. Several wells allowed for controlling the interpretation of each top sediment unit and performing the time-to-depth conversion. These interpretations produced a 3D basin model, which was used to understand the origin of the Ombilin Basin.

3.1. Digital Elevation Model (DEM)

The surface structures of the basin and its surroundings were interpreted using a high-resolution Digital Elevation Model (DEM). The Digital Elevation Model (DEM) is a tool to portray the information of the earth's surface including its relief, elevation, and other topographic information captured by satellites and other aerial tools. It is often used to extract the linear aspect of the Earth's surface or often called as lineaments, which represent the occurrence of geological or geomorphological phenomena (Clark & Wilson, 1994).

The Digital Elevation Model (DEM) data of the area are comprised of several 1:25000 raster maps that are available on the website https://big.go.id. The data has been built by the Indonesian Geospatial Information Agency (BIG) from several sources including IFSAR (5m resolution), TERRASAR-X (5m resolution), and ALOS PALSAR (11.25m resolution). The reference vertical datum is EGM2008 while the spatial resolution is 0.27-arcsecond or 8.25 meters. In order to combine several raster maps, the ArcMap (Esri's ArcGIS) geospatial processing software was used.

Interpreting the structural aspect on the surface topography needs a more straightforward procedure. Therefore, hill shading of DEM data is necessary to provoke a better impression of topographic relief to estimate the tectonic response of the surface.

The previously combined maps were then exported to the free and open-source cross-platform called QGIS to create the hill-shaded effect. The QGIS software was utilized since it is capable to generate a combined multi-directional hill-shaded image that comes from four different lighting directions into one raster file. This was applied to avoid the topography bias as the traditional shading light direction only coming from one azimuth direction, usually north-west light direction (Abdullah et al., 2010).

Since the study area experienced several tectonic events that affected a complex morphology, the light effects from azimuth 45˚, 135˚, 225˚, 315˚ were applied. Finally, manual lineament extraction by visual interpretation was conducted to the preconditioned DEM data to identify the geomorphology variations, such as the lineament of valleys, ridges, the rivers offset, and the boundary of a rock unit that might indicate the existence of a geological structure on the surface and subsurface. Furthermore, the lineament extraction in correlation with the regional geology was used to assist the prediction of structural geology that might exist in the subsurface of the Ombilin basin.

3.2. Seismic data

This study utilized the two-dimensional pre-stack time migrated (PSTM) seismic lines with a total of 84 seismic lines that cover mostly the Sinamar sub-basin (Figure 7). The total length of the available seismic lines is 874,244.69 meters including the total length of interpretable seismic lines is 733,871.94 meters. The display of the available seismic lines is in one-way-time (OWT) and the velocity value is 2 m/sec.

Overall, within thirty-five years, 55 SW-NE and 29 NW-SE trending lines have been recorded in three different periods of seismic surveys. In the period of 1981 until 1983, there are 61 seismic lines were recorded while in the second period between 2010 and 2011 only 19 lines. The average depth of these seismic lines was 3000 ms (OWT), despite 3 deeper lines of 6000 ms (OWT) in the last period between 2015 and 2016 were recorded. The seismic survey was provided by PT. Rizki Bukit Barisan Energi.

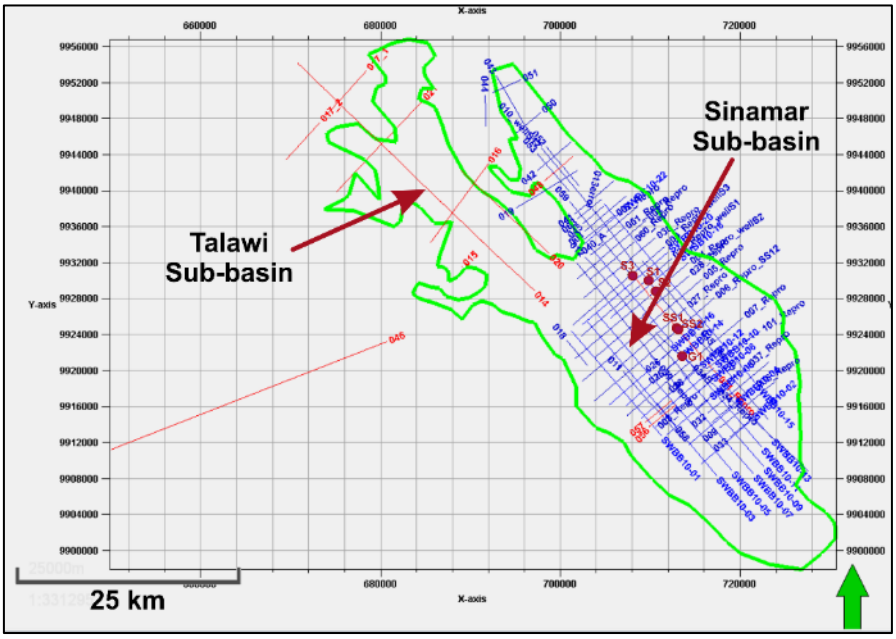

Figure 7. The availability of two-dimensional seismic lines at the Ombilin Basin. The seismic lines mostly cover the Sinamar Sub-basin. The total length of good-interpretable seismic lines is 733,871.94 meters (blue lines) while the length of the poor-quality seismic line is 140,372.75 meters (red lines).

3.3. Well data

A Total of six exploration wells have been drilled in this basin of which four wells are vertical and the other two are inclined. The first and deepest well is the Sinamar-1 with total a measured depth of 9902 ft (3018.13 m) at a surface elevation of 679.4 ft (207.08 masl) penetrating until the Top Lower Sangkarewang unit (Koning, 1985).

There are eight well markers available to determine the top of each sediment unit: based on chronostratigraphy consisting of the Brani Formation, the Sangkarewang Formation (Lower and

Upper), the Sawahlunto Formation, the Sawahtambang Formation (Lower, Middle, Upper), and the Ombilin Formation. The well data, including well markers, were provided by PT. Rizki Bukit Barisan Energi, together with the seismic data.

3.4. Seismic interpretation

To establish the correct correlation between the seismic lines, each seismic line was calibrated by shifting the depth of vertical geometry. This was conducted to establish a good correlation between the seismic lines. Moreover, the seismic to well tie data in this study used the data from PT. Rizki Bukit Barisan Energi. The interpretation of 2D (two-dimensional) seismic data was conducted using Petrel Software (Schlumberger).

To simplify the interpretation, only three well markers from the provided data were utilized. These are the top marker of Brani, Sangkarewang, and Sawahtambang formations. The interpretation of Sawahlunto Formation was combined to the Sawahtambang Formation because the interface between both formations is difficult to determine in the seismic section. Since this basin overlies the Pre-Cenozoic rocks that comprise of meta-sediment, volcanic materials, and granite, the interpretation of the top basement was conducted by recognizing the unconformity from the ceased reflectors and determine the chaotic seismic facies. Therefore, in total, four horizons were interpreted to model the basin.

The published wireline logs and provided markers were used to control the interpretation. The Sawahtambang Formation that thins towards the south is recognizable in the seismic section and can, therefore, be used as a seismic control. The interpretation was begun by using a seismic line that crosses the oil well. Then, the composite seismic lines were constructed to correlate the interpreted horizons. Meanwhile, the boundary of each sediment unit as well as the identification of geological structures such as fault was also established by recognizing the terminations of seismic reflectors. Finally, the interpreted grid of 2D seismic lines was then interpolated to make a 3D surface of each horizon.

Isopach or thickness maps of the main stratigraphic units were then created from the 3D surface interpolation. The thickness maps were created by calculating the true stratigraphic thickness (TST) of each stratigraphic unit. The true stratigraphic thickness calculation is important to avoid misleading information from a true vertical thickness (TVT) of the deviated boreholes and dipping beds. In general, the operation consists of measuring the perpendicular strike direction of two different bedding units.

3.5. Time-to-depth conversion

Time-to-depth conversion is an essential process in building a geological model that uses seismic data as the main tool to interpret the geometry of the subsurface. Since the seismic measurements are made in time and the wells are drilled in depth, an inaccurate execution may lead to many errors: miss the targeted depth of reservoir zone, wrong volumetric calculation, etc. Depth conversion in geological modeling can be simple or complex depending on how much data are available as well as the play scenario. Many methods can be utilized, such as direct time-depth conversion, depth conversion using the velocity model, and using checkshot data (Francis, 2018a). Considering the available time for this project and because it is unclear which checkshot data is reliable, the direct time-depth conversion method was selected.

Francis (2018b) explained the step by step the direct time-depth conversion. In this study, the depth information of each stratigraphic unit that has been known from the available well markers was compiled. Then, the time information where those markers seated in the seismic were also collected.

Subsequently, the linear function of seismic time versus depth of each unit (top of each stratigraphic unit) was established (Figure 8).

The distribution of the well data in the graphs (Figure 8) depicts a small mean residual difference and low standard deviation. This evidences a good depth conversion model and indicates low uncertainty in the obtained depth. Because of the depth of sediment units is different at each well, in order to avoid distortion, each function was applied to each stratigraphic unit separately. It is a simple multiplication operation to each stratigraphic unit to produce a depth-domain surface.

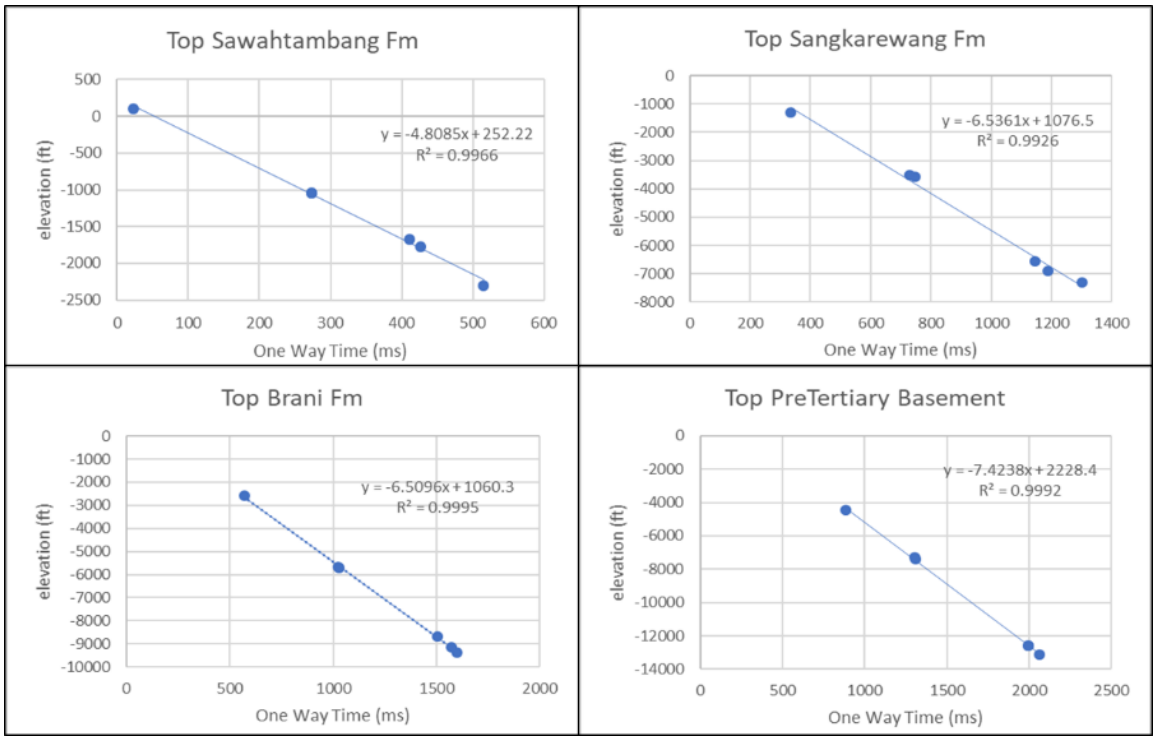

Figure 8. The linear function of seismic time versus depth of each interpreted stratigraphic unit. A total of six wells were utilized to produce the linear function. The graphs show a good spatial distribution of time versus depth on each stratigraphic unit. The depth conversion was applied by simply multiplying the function to each time-domain surface.

4. Result

4.1. The surface structural trends of the Ombilin Basin

Lineaments were mapped on the DEM images using the multi-directional lighting effects of hill-shading. Several features such as lineament of several straight valleys, ridges, and the offset of rivers can be identified.

There are at least four major lineament trends that were mapped in the study area: NW-SE, E-W, N-S, and NE-SW (Figure 9). The most prominent lineament is the NW-SE trending that dominates the Ombilin Basin and Sumatra as a whole. The high density of this trend can be found on the East of the basin, on the south near Bakardalam, at the Talawi, and along the west-southwest (Figure 9). This NW-SE trend around the Solok and Bukit Gadang is the trend of an active Sumatran Fault System (Figure 9). In the Ombilin basin itself, this trend can be found from the Mount Malintang crossing through the basin and ceases on the southeast of the basin before reappearing at Bakardalam (Figure 9).

These NW-SE trends are deflected towards the east and amalgamated with the E-W trend in some areas. This can be seen near the Sungailangsat, Barungbarung Rendah, and most noticeable at

Lubukanbacang (Figure 9). The N-S trends mainly found within the Ombilin Basin, in Talawi, Palaular, Sijunjung, and in the southern of Sinamar. The Talawi and Sinamar sub-basins are bisected by this N-S trend. The last trend is the NE-SW trend, which looks like a minor trend in this area. It is generally detected at Muara and on the SSW of the basin.

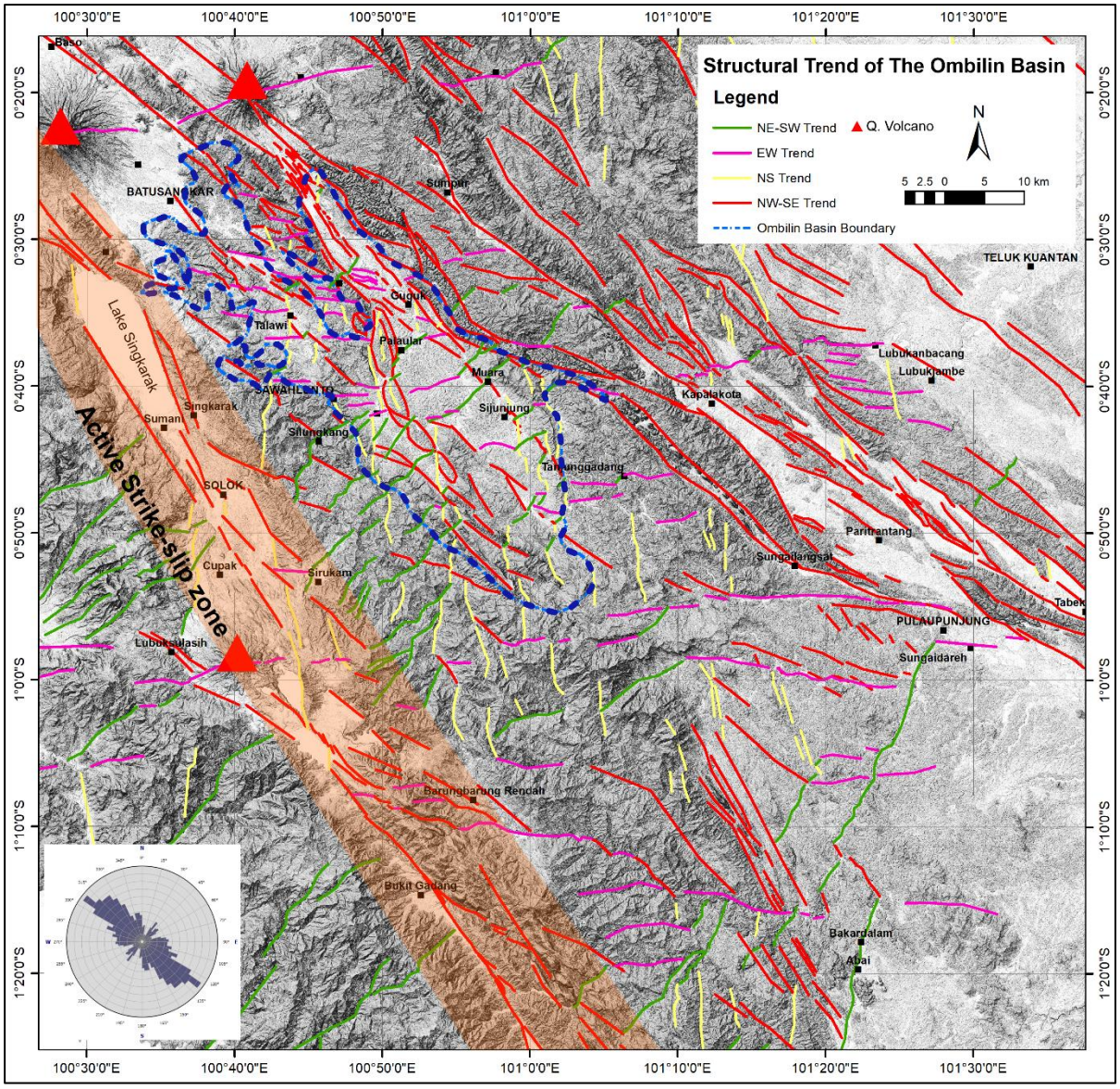

Figure 9. The structural trend of the Ombilin Basin from the lineament extraction of the Digital Elevation Model (DEM) using multi-directional hill shades: from azimuth 45˚, 135˚, 225˚, 315˚. The Ombilin Basin is dominated by the NW-SE trend (red line) and N-S (yellow line), also some other minor trends, such as the E-W (pink line), and the NE-SW (green line).

4.1.1. The Lineaments at the Ombilin Basin in comparison with the geology

The lineament interpretation of valleys, ridges, and rivers were then compared to the well-known geological features as mapped by Silitonga & Kastowo (1975), Koning (1985), and Situmorang et al. (1991).

The structures in the basin area are diverse but mainly NW-SE trending in both the Talawi and Sinamar sub-basins. The E-W and N-S trends also cover the Talawi sub-basin as well as in the Sinamar sub-basin in addition to the NE-SW trend that crosses the sub-basin center (Figure 9). The NW-SE trend is

identical to the Takung Fault on the eastern edge of the basin as well as the Sumatran Fault System on the west (Figure 11). Moreover, the lineament of the Sitangkai fault together with Palangki Anticline and Batikin Anticline also belongs to this NW-SE trend. Geologically, the predominantly NW-SE trend in this basin and Sumatra is an indicator that the major stress direction is from the NE-SW direction.

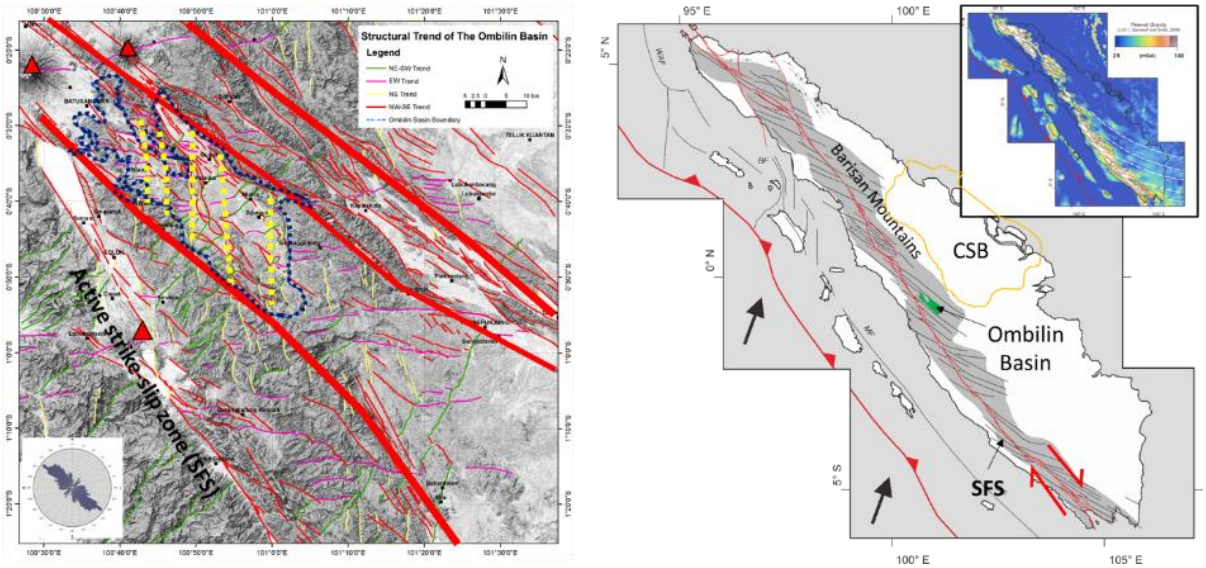

Figure 10. The NW-SE trend in the research area in comparison with the lineament of basement fabrics from the gravity data interpretation (after Sutrisno et al., in prep). The N-S trend looks like a series of NS fault structures.

In comparison to the orientation of inherited basement fabrics from the gravity data interpretation (Figure 10) by (Sutrisno et al., in prep), the NW-SE trend in this area is similar to this orientation. Therefore, by excluding the orientation of the Sumatran Fault System, the NW-SE trend within the research area is interpreted as the trend of the basement structure.

The distinct anastomosing pattern (Figure 11) in the Sinamar Sub-basin is mainly within this trend. This anastomosing pattern appears from the southeastern edge of Bukit Tungkar (near Palaular) and ceases to the southwest of Palangki anticline. It resembles the pattern along with the karst topography in the east that is parallel to the Takung Fault. The anastomosing pattern in the Palaular is somewhat parallel to the N-S trending before it deflects away following the NW-SE trend to the southeast.

Meanwhile, the N-S trend within the Ombilin Basin is also interpreted as a series of N-S structures that are bounded by the inherited basement structure. The Tanjung Ampolo fault (Figure 11) and the southeast boundary of the basin are recognized by this N-S trend while the other trends such as E-W and NE-SW do not represent any well-known structures but may perform as a shear and fault zone.

Overall, the lineament extraction assists the delineation of structural geology that might exist in the subsurface and identification of large scale and long-lived structural features of Sumatra that controlled the development of the Ombilin Basin. The new features that were identified in this study were then used to update the previous regional geological map of the Ombilin basin, which can be seen in Figure 11.

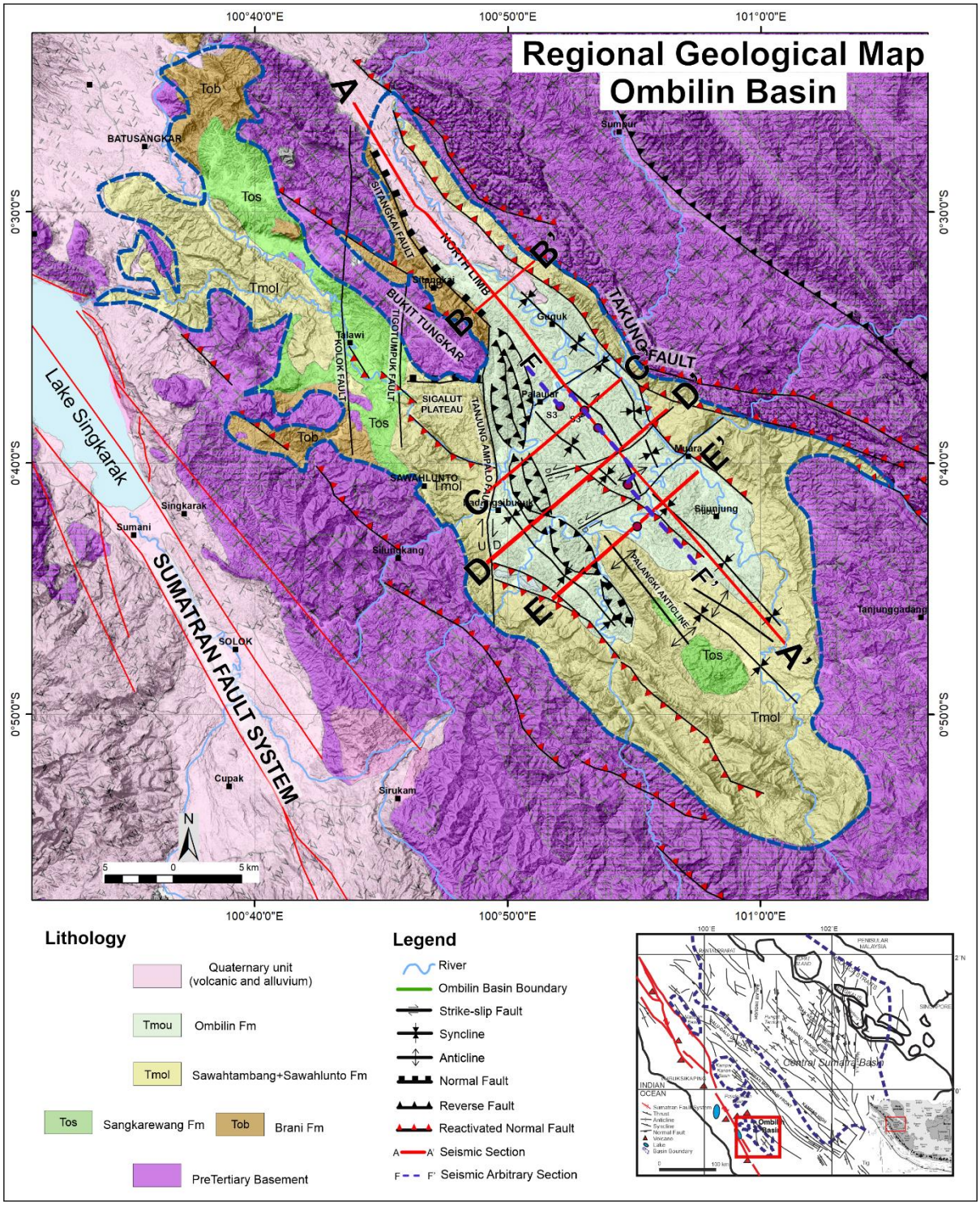

Figure 11. Regional Geological map of the Ombilin Basin overlying the topographic map of the Digital Elevation Model (DEM) modified from Silitonga & Kastowo (1975), Koning (1985), *and* Situmorang et al. (1991). *The fault lines were updated using the interpretation of the Digital Elevation Model and the seismic survey that was used in this study. The older strata of Paleocene- Eocene Brani and Sangkarewang formations represented by brown and dark green, respectively, are mainly exposed in the Talawi area while only some position of Sangkarewang Formation exposed in the southern part of Sinamar area. From this map, we can determine that different rates of erosion affected the Ombilin Basin.*

4.2. Basin geometry

The sub-rhombohedral Ombilin Basin consists of two sub-basins: Talawi and Sinamar. The NW-SE is the major structure direction in the Ombilin Basin represented by folds, reverse, and normal faulting as well as the anastomosing fault pattern in the Sinamar sub-basin (Figure 11). The N-S and NE-SW

trending structures are the second and third, respectively. The oblique-slip faults with dextral motion belong to the N-S trend. The last pattern is the NE-SW trending strike-slip faults that have sinistral motion.

4.3. Ombilin Basin structure

In bird's-eye view, the northeastern part of the basin is bounded by the NW-SE trending reverse fault, the Takung Fault, in which the pre-Tertiary rock thrust onto the Tertiary sediments. This fault lies from the northeastern edge of the basin to the southwest and slightly deflected to the east in the middle basin before it deviates back to the NW-SE trending to the southwestern of the basin (Figure 11).

On the other hand, the southwestern and the southeastern parts of the basin are not fault-bounded from the DEM (Figure 11). The segmented reverse faults are, indeed, can be seen on the southwest outside the basin but not become the boundary of the Ombilin Basin based on the DEM interpretation (Figure 11). The northeastern part of the basin is unconformably overlain by the Quaternary volcanic materials which cover some of the Sinamar sub-basin (Figure 11).

Reminiscing that the Ombilin Basin consists of two sub-basins separated by a basement high, these sub-basins are also bisected by the N-S trending fault, the Tanjung Ampalo Fault (Figure 11) (Koesoemadinata & Matasak, 1981; Koning, 1985; Situmorang et al., 1991; Barber et al., 2005). These two features, the Tanjung Ampolo Fault and the basement high, are then become the main separator of Talawi and Sinamar sub-basin.

Two N-S trending faults (Figure 11) are also visible in the Talawi sub-basin resembling step-faults-like features together with the Tanjung Ampalo Fault (Figure 11). According to Situmorang et al. (1991), these faults, from the northwest to the southeast are recognized as Kolok Fault and Tigotumpuk Fault.

Since the structural modeling of the subsurface was only conducted in the Sinamar sub-basin, which is the down-thrown part, the next section is focused on this sub-basin, leaving aside the Talawi sub-basin.

4.4. Seismic interpretation of the Sinamar Sub-basin

In general, the seismic reflections show the overlain and underlain strata were deformed in the same manner. Several seismic signatures are recognized from the interpretation, for example, the seismic facies, the geometry of the reflection, and the reflection termination. The inline seismic section AA' (Figure 12) depicts the geometry of the Ombilin Basin fill which has divergent reflection configuration characterized by a wedge-shaped. The divergent reflectors are an indication that progressive tilting of a depositional surface occurred while the deposition of each sediment unit

The seismic facies of the Tertiary units in the southeastern area (Figure 12) is characterized by chaotic reflectors (Figure 12) presumably as the result of high deformation in this area. Through the northwestern part, the reflector continuity becoming low to moderate with the internal configuration of wavy to subparallel (Figure 12), especially in the middle part characterized by high frequency and moderate to high amplitude (Figure 12). Within the distal part of Sawahtambang and Sangkarewang Formation (green box in Figure 12), the seismic reflector depicts presumably an alluvial-fan or fan-delta deposit from a local horst block.

The truncation of seismic reflectors in the southeastern part (Figure 12) defines the establishment of the angular unconformity between the Sawahtambang and Sawahlunto formations and the underlain Sangkarewang as well as Brani formations. From the seismic profile AA' in Figure 15, the Sawahtambang Formation is thickened towards the northwest where part of its unit unconformably lies onto the basement rock.

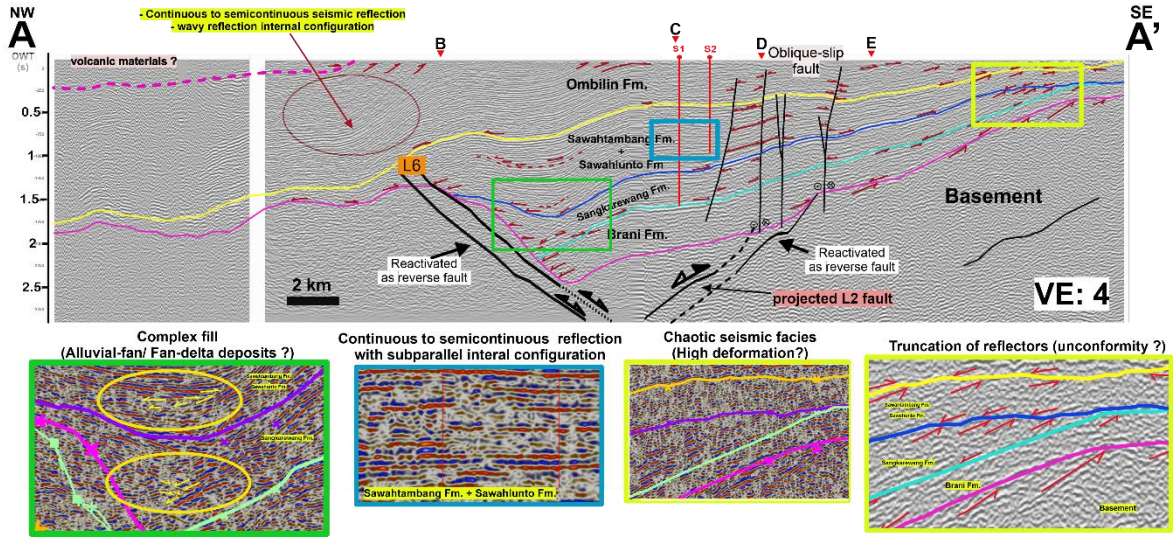

Figure 12. The Inline seismic section (section AA') of the Sinamar Sub-basin shows the interpretation of seismic reflection termination and overview of seismic facies. In general, several features can be identified such as the unconformity from the truncation of the reflectors (yellow box), the possible alluvial-fan or fan-delta deposit in the middle part of the section (green box) and the reflection configuration as well as the continuity of the reflectors (blue box). Location see Figure 11.

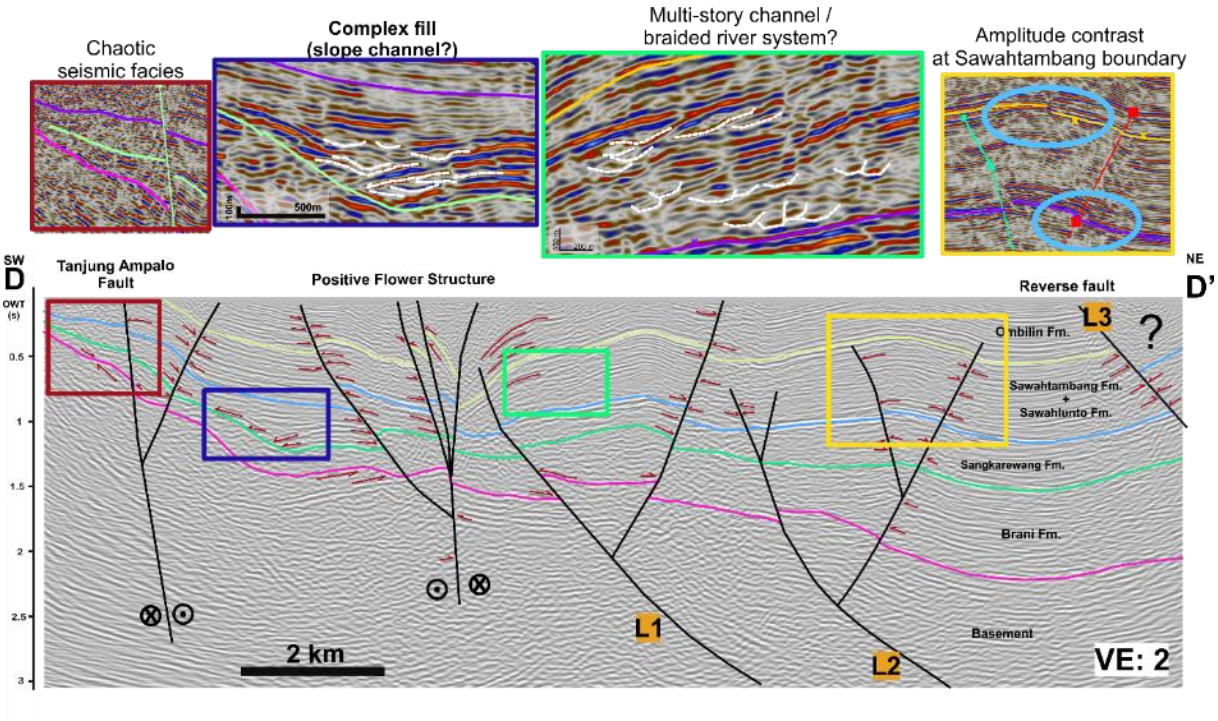

Figure 13. The crossline seismic section (section DD') of the Sinamar Sub-basin shows the interpretation of seismic reflection termination and overview of seismic facies. In general, several features can be identified such as the chaotic seismic facies (red box), the possible slope channel within Brani Formation (blue box) the multi-story of the braided river system (green box), and the interface of Sawahtambang Formation by amplitude contrast (yellow box). Location see Figure 11.

Meanwhile, from the crossline seismic section DD' (Figure 13), the chaotic seismic reflectors denote the southwestern part suggesting high deformation affected this area while the low to moderate reflector continuity represents the middle to the northeast area. Other features can also be identified from this seismic section such as the positive flower structure, the possible alluvial slope channel within the Brani Formation, the multi-story of braided river system within the Sawahtambang Formation, and the amplitude contrast as an indication of the interface of the Sawahtambang Formation with the overlying and underlying units (Figure 13).

The depositional environment in particular the Ombilin Formation can also be identified from section FF' (Figure 14). The seismic facies within both formations indicate a lateral variation from the northwest to the southeast which is evidenced by the changing from the semi-continuous high amplitude to semi-continuous low amplitude (Figure 14). Moreover, the well correlation of the units (Figure 14) shows that the shales content of the Ombilin Formation in the northwest area is lower than the southeast area. This gives the information that presumably the proximal-medial to distal area of this formation started from the northwest through the southeast part of the section (Figure 14).

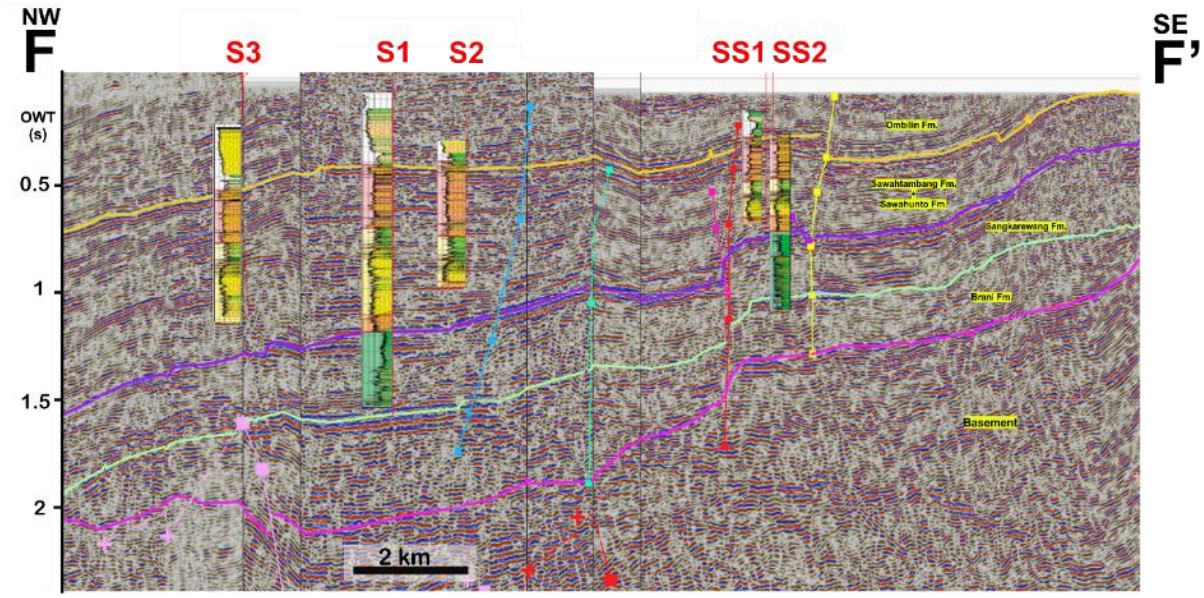

Figure 14. The arbitrary seismic section in NW-SE orientation (section FF') of the Sinamar Sub-basin shows the identification of each top formation using wireline logs by Habrianta et al. (2018). The yellow and green color fill in the wireline logs represents the sand and shale dominated lithology, respectively. Location see Figure 11

Seismically the boundary between each Tertiary unit is not always straightforward. The identification of each top formation was assisted using the wireline logs from Habrianta et al. (2018). From section FF' (Figure 14), the boundary between the Sangkarewang Formation and the Sawahtambang Formation is denoted by the shift of the Gamma-Ray log. The high value of the Gamma-Ray log at the low seismic amplitude represents the lacustrine shale of Sangkarewang Fm while the low value of Gamma-Ray at moderate to high seismic amplitude represents the fluvial clastic sediments of the Sawahtambang Formation. The interface between the Oligocene Sawahtambang Formation and the Early Miocene units of the Ombilin Formation (Figure 14) is denoted by the change of Gamma-Ray pattern from cylindrical blocky shaped to the funnel-shaped divided by the shale break.

4.5. The Interior Structure of the Sinamar Sub-basin

The large Sinamar Sub-basin extends from the southeast of the mount Malintang towards the south-southwest with a total area around 840 km2. In this depocenter, three Tertiary sediment units outcrop unconformably to each other, the Miocene Ombilin Formation, the Oligocene Sawahtambang Formation, and the Paleocene-Eocene Brani Formation (Figure 11). The Ombilin Formation is

unconformably bounded by the Brani Formation on the northwest and partly covered by a Quaternary material of inactive Malintang volcano (Figure 11).

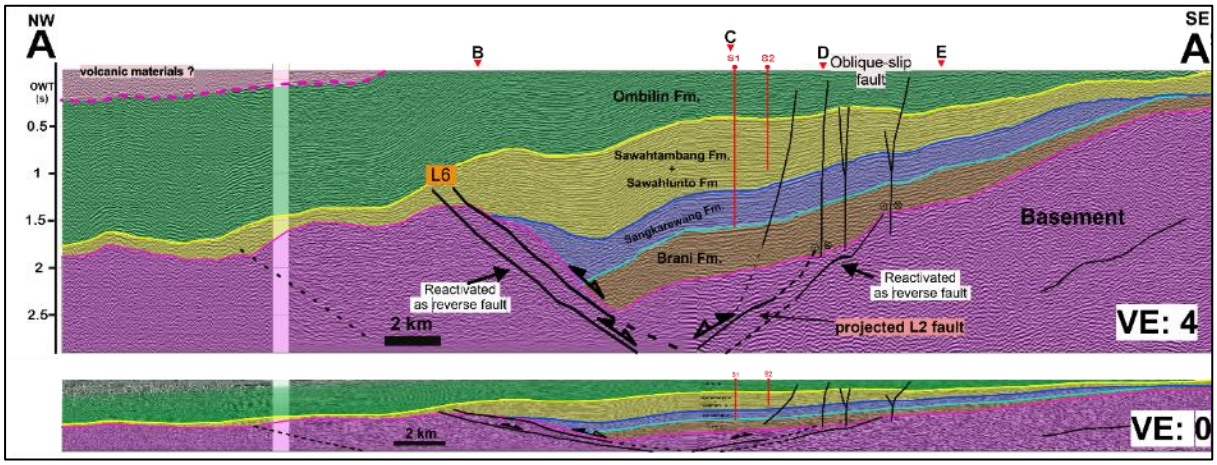

Figure 15. The Inline seismic section (section AA') of the Sinamar Sub-basin. The thickest sediment or the deepest basin center is recorded in this seismic section. The sediments are wedding to the northwest direction. The deepest well of Sinamar-1 (S1) is crossed by this inline section. Location see Figure 11.

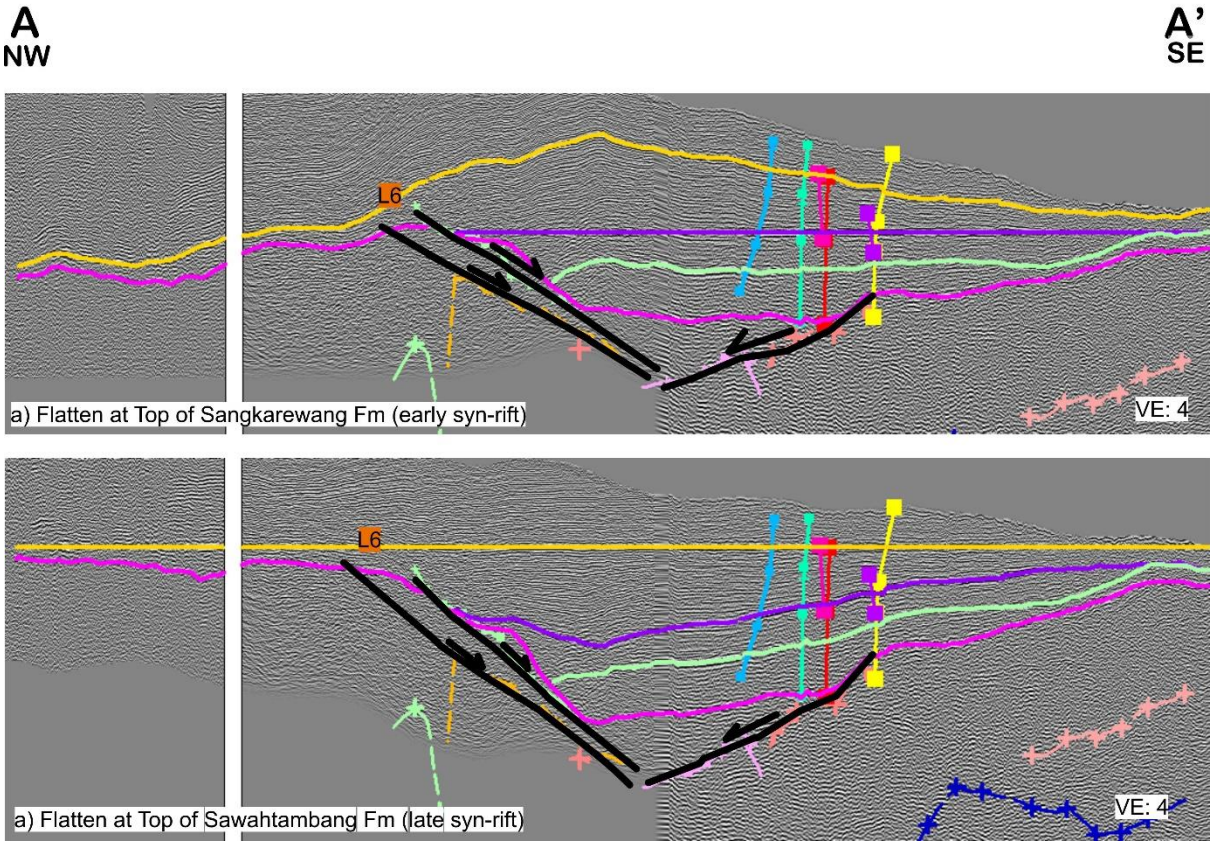

Figure 16. A) The flatten horizon at the top of the Paleocene-Early Eocene Sangkarewang Fm. (the early syn-rift phase). B) The flatten horizon at the top of the Oligocene Sawahtambang Fm (the late syn-rift phase). The deepening of the half-graben was controlled by the fault L6 on the NW side that acted as the master fault.

The sub-basin geometry is narrow from the northeast and widening to the south. Based on the seismic profile (Figure 15), it is comparable to a half graben-like structure by its asymmetrical geometry. The early Paleogene sediments seem accumulated from a wider area in the SSW thicken towards the

narrower area of the North Limb in the northeast and disappears beneath the Mt. Malintang (Figure 15).

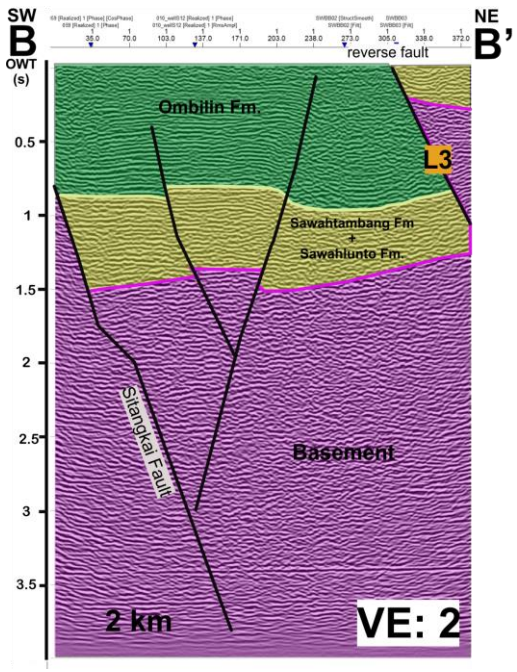

Figure 17. The seismic cross section of SW-NE direction (section BB') is in the North Limb area. The normal fault on the southwest is the Sitangkai Fault. The surface and subsurface deformation is less likely affecting the area instead of this place is the narrowest area of the Sinamar Sub-basin. Only several folding structures exist, and the sediments are gently dipping to the northwest. VE is vertical exaggeration. Location see Figure 11. The fault L3 in this section is the component of Takung Fault of which portion of the Sawahtambang Formation (Oligocene) is thrust over the younger basin fill

The structural components in the Sinamar are diverse and include folds, oblique-slip, reverse, and normal faults. As mentioned in the previous section (Section 4.3), the sub-basin is bounded in the Northeast by the reverse fault component (L3 in Figure 17) of the Takung Fault along which portion of the Sawahtambang Formation (Oligocene) is thrust over the younger basin fill. To the west of this fault, the basin suddenly deepens and shallowing to the southeast (Figure 21). The southwestern edge of the North Limb is bounded by the Sitangkai Normal Fault in the footwall of which the Brani Formation crops out. Although the North Limb is much narrower than the rest of the basin, it is relatively little deformed. Only several folds exist, and the sediments are gently dipping to the northwest (Figure 17).

The development of the graben and the rifting phase can also be studied in Figure 15. In the early syn-rift, the development of the half-graben was controlled by the fault L6, which acted as the master fault. From the map view, the fault L6 is the N-S trend structure. This allowed the deposition of the Paleocene-Early Eocene alluvial fan of Brani formation from the local horst blocks interfingering with the lacustrine shale of Sangkarewang formation. Then, the normal faulting of L6 continued allowing the deposition of the Late Eocene fluvio-deltaic that contain coals of Sawahlunto and the Oligocene braided river sandstone sediments of Sawahtambang formations. At the end of the deposition of Sawahtambang formation, the normal faulting of L6 started to stop allowing the Sawahtambang formation deposited further to the NW unconformably onto the basement rock to fill up the graben. Therefore, the Sawahlunto and Sawahtambang formation are categorized as the late syn-rift deposits. The last was the deposition of marine shale of the Ombilin Formation in the transgressive phase as post-rift sediment. Flattening of the horizon in (Figure 16) also shows that the syn-rift deposition was indeed controlled by the fault L6 on the NW side that acted as the master fault. The angular unconformity that is found at the basin edge in the SE area indicates the occurrence of erosion while the deposition of Sawahtambang and Ombilin formations.

The NW-SE inherited basement structures that are recognized from the surface interpretation is represented by the fault L1, L2, L3, and L4 (Figure 18 & Figure 19). These reverse faults were initially the normal faults that were reactivated during the basin inversion in the Mid-Miocene and Plio-Pleistocene tectonic phase. These faults are characterized by gentle dipping fault to the northeast followed by the conjugation of back thrusting (fault L1 and L2 in Figure 19 also L4 in Figure 20). This influenced the development of several folds (anticline and syncline) on the surface. The Palangki

anticline (Figure 20) is the most recognizable folding structure on the surface where the unconformity between Miocene Ombilin Formation and Oligocene Sawahtambang Formation is outcropped.

Careful mapping of the surface structure in the current study found the most distinct feature in the Sinamar. It is the NW-SE trend anastomosing pattern on the east of Tanjung Ampalo Fault. The anastomosing fault zone is a strike-slip fault artifact as a result of shear interconnections that generally parallel to the basement fault (Dooley & Schreurs, 2012). From the identification of ridges and valley lineaments in Figure 9, it is seen that the chain of several antiforms is developed from the edge of Sitangkai fault and Tanjung Ampalo near Palalular around 4 km wide and narrowing to the west of Palangki Anticline. At the Palaular area, the trend of this anastomosing is N-S and gradually changes to the NW-SE trend to the west of Palangki Anticline.

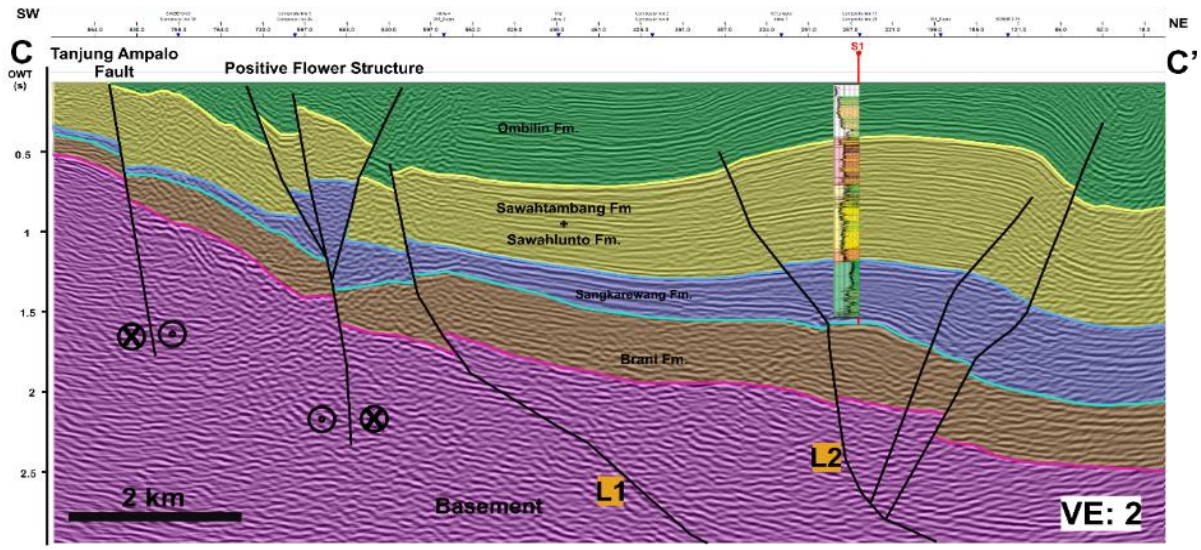

Figure 18. The crossline seismic section (section CC') of the Sinamar Sub-basin. The fault L1 and L2 are the NW-SE inherited basement fabrics. The Tanjung Ampalo Fault is the N-S oriented structure as the master fault during the rifting phase, which later reactivated as dextral strike-slip during basin inversion in Mid-Miocene and the development of back-thrusting. The anastomosing fault pattern that is found from the surface interpretation created a positive flower structure during the basin inversion. Location see Figure 11.

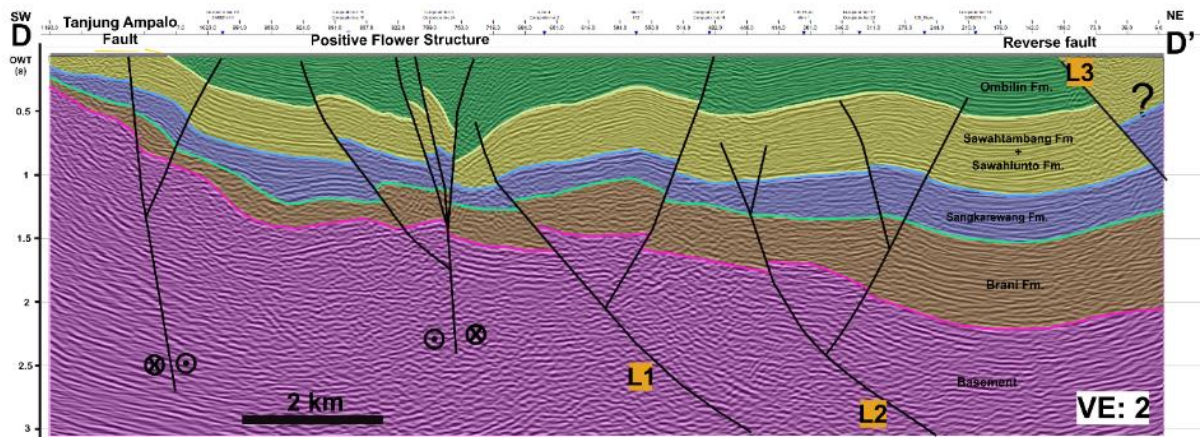

Figure 19. The crossline seismic section (section DD') of the Sinamar Sub-basin. The fault L1, L2, and L3 are the NW-SE inherited basement fabrics that reactivated as reverse fault during the basin inversion (Mid-Miocene). The Tanjung Ampalo Fault is the N-S oriented structure as the master fault during the rifting phase, which later reactivated as dextral strike-slip during basin inversion in Mid-Miocene and the development of back-thrusting. The anastomosing fault pattern that is found from the surface interpretation created a positive flower structure during the basin inversion. Location see Figure 11.

Throughout the seismic section (Figure 18,Figure 19, and Figure 20), this anastomosing fault pattern created a positive flower structure as an indication of the transpressional setting that affected the study area. The fault is characterized by a peculiar seismic dead zoned in a narrow shear zone of up to 2 km wide. In the previous study by Koning (1985), it is known as Suo Fault, which is located east of the Padangsibusuk area to the west of the Palangki Anticline.

The seismic section (Figure 18 & Figure 19) across the region of anastomosing faults also shows a highly deformed fault zone with pop-up structures. These pop-ups are bounded by several sub-vertical reverse faults (Figure 18 & Figure 19). In the surface map (Figure 11), these reverse faults define the geometry of the pop-ups, which is sigmoidal to an elongated lozenge.

The positive flower structure (Figure 18 & Figure 19) is rather an asymmetry. The asymmetry geometry of theses structure is indicated by a steeply dipping reverse fault on one side and more shallowly dipping on the other side. The reverse faults are more developed in the northern part (four faults identified) than the southern part (two faults) indicating the irregularity of pop-ups development (Figure 11). Localized rollover anticlines are also identified in some areas of the pop-ups (Figure 19). The initiation of the Barisan Mountain together with the activation of the Sumatran Fault System since the Mid-Miocene yielded the basin inversion and rejuvenation of previous faults also the new conjugate faults with series of anticline and syncline. Because this anastomosing pattern and other strike-slip components cross the youngest strata, it is interpreted to occur in the later tectonic phase (Plio-Pleistocene).

It is beyond the scope of this report to discuss the kinematic of this strike-slip component. However, comparing the analog model by McClay & Bonora (2001) the development of these pop-ups was influence by the block faulting of the dextral movement of the Tanjung Ampalo Fault results in the sinistral motion of western pop-ups zone (Figure 11). Towards the south, these pop-ups deflected to the NW-SE direction (Figure 11). Further study might be needed to investigate the kinematic of this anastomosing pattern.

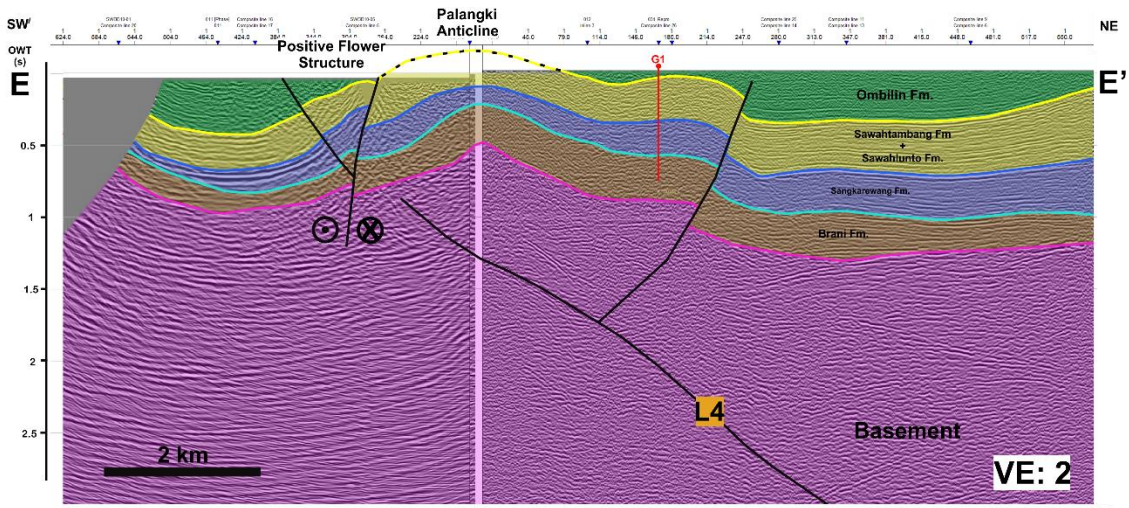

Figure 20. The crossline seismic section (section EE') located in the southeast of the Sinamar Sub-basin. The fault L4 is the NW-SE inherited basement fabrics. Little deformation affecting the area due to its location in the basin edge. The fault L4 reactivated as reverse fault during the inversion (Mid-Miocene) creating Palangki Anticline where some portion of the Oligocene Sawahtambang Formation is exposed. The anastomosing fault pattern that is found from the surface interpretation created a positive flower structure during the basin inversion. Location see Figure 11.

4.6. The depth structure maps

The seismic interpretation that was conducted in this study was used to generate four depth structure maps, includes the top of Basement (Figure 21), top of Brani Formation (Figure 22), top of Sangkarewang Formation (Figure 23), and top of Sawahtambang Formation (Figure 24).

The depth structure of the Pre-Tertiary basement (Figure 21) in the Sinamar sub-basin depicts that the N-S and the NW-SE oriented faults dominate this sub-basin. It is distributed from Guguk to the southern area (Figure 21). These faults are similar to the structural trend on the surface. From this map (Figure 21), the deepest depocenter around 5 km depth is also discovered, which is in the area of Palaular and Guguk bounded by the Takung Fault.

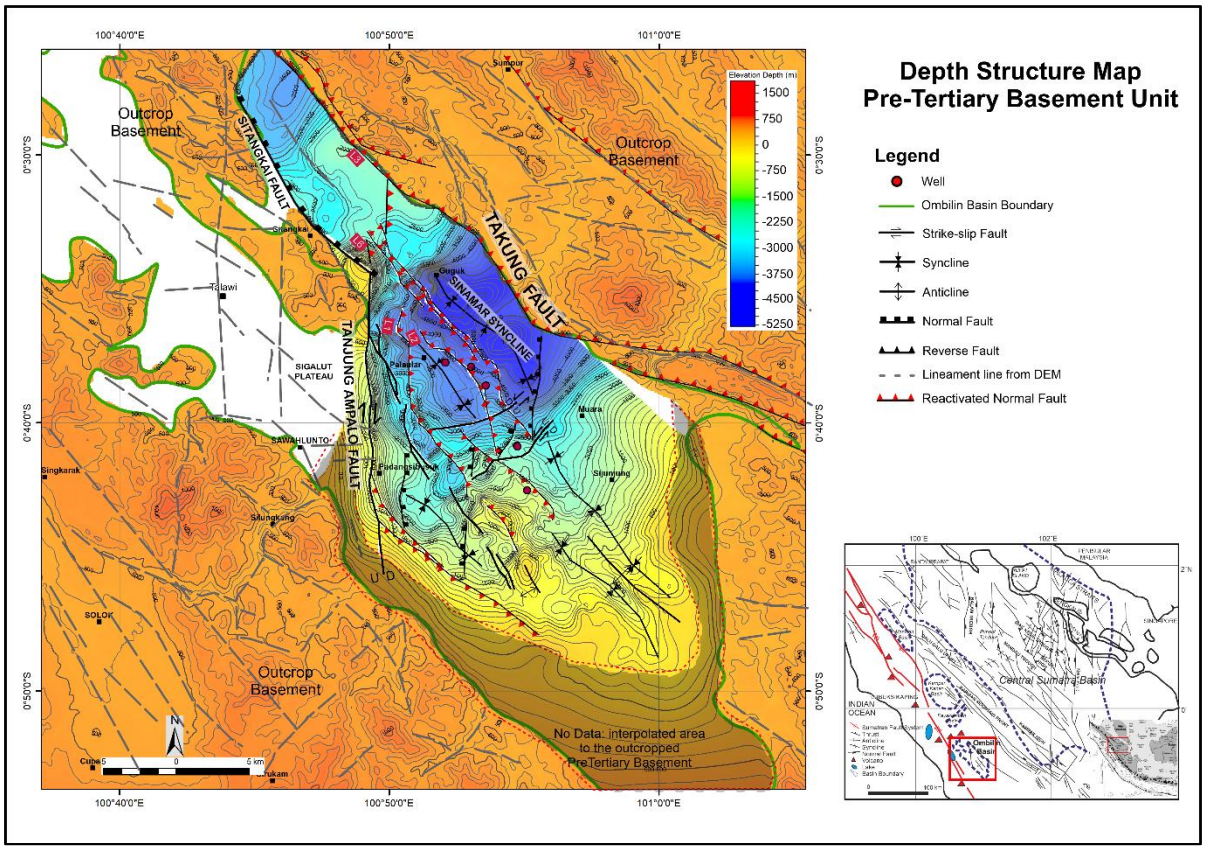

Figure 21. The depth structure map of Top Pre-Tertiary Basement that has been combined with the basement outcrop (orange to red color) from the surface geology map. The basement is dominated by the N-S and NW-SE trend structure. The deepest depocenter is near the Guguk area on the south of Takung Fault.

The N-S and NW-SE oriented faults are still established up to the top of Sangkarewang Formation (Figure 23) while the top of Sawahtambang Formation (Figure 24) is only dominated by the NW-SE faults. This is because the N-S fault that controlled the rifting phase started to stop at the end of the deposition of the Sawahtambang Formation in the Late Oligocene.

Another structural feature that can be determined in the Sinamar is NE-SW trending sinistral strike-slip faults (Figure 23) near the Muara area. These faults penetrate all sediment units up to the surface, which can be seen from the seismic section in Figure 15. They are relatively parallel to each other along with the orientation of the river (Figure 11). Meanwhile, the N-S dextral oblique-slip of the Tanjung Ampalo Fault, which is the rejuvenation of normal fault during the Mid-Miocene and the Plio-Pleistocene inversion, is easily identified from the Sawahtambang map (Figure 24).

The anastomosing pattern that is found from the surface interpretation diminishes through the basement depth. The comparison can be seen from the surface map (Figure 11) and the Basement depth map (Figure 21). The fault is presumably associated with the NW-SE oriented inherited basement fabrics within the central Ombilin Basin that were reactivated as transpressional faults during the Plio-Pleistocene tectonic phase.

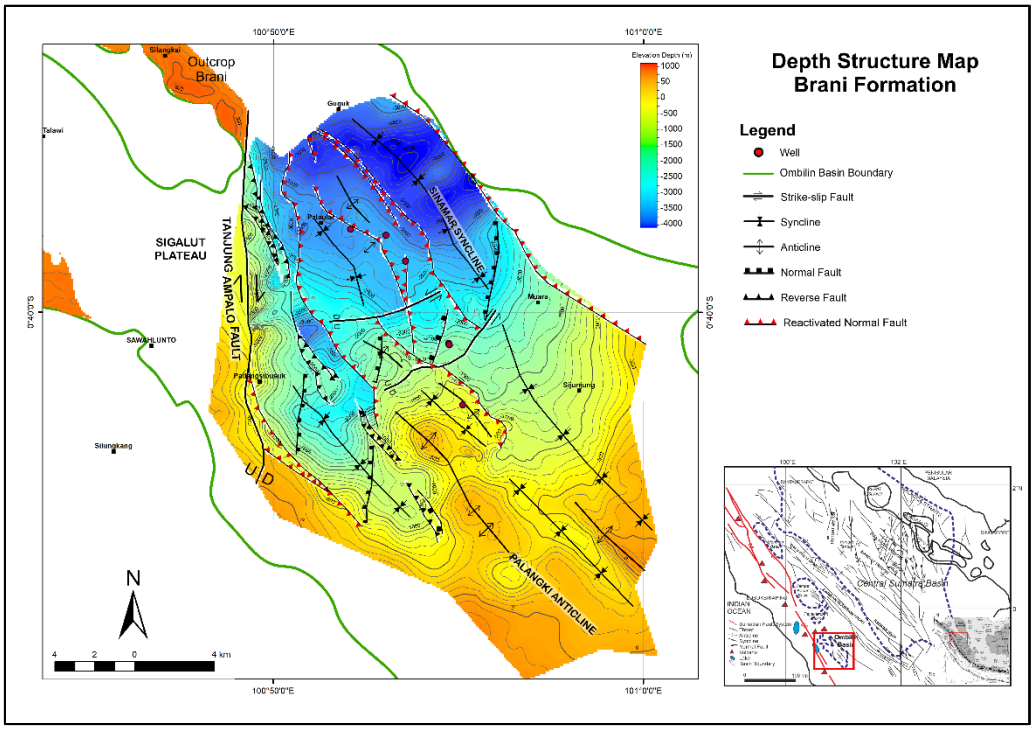

Figure 22. The depth structure map of Top Brani Formation. The structure is dominated by the N-S and NW-SE trend faults. The deepest depocenter is near the Guguk area on the south of Takung Fault.

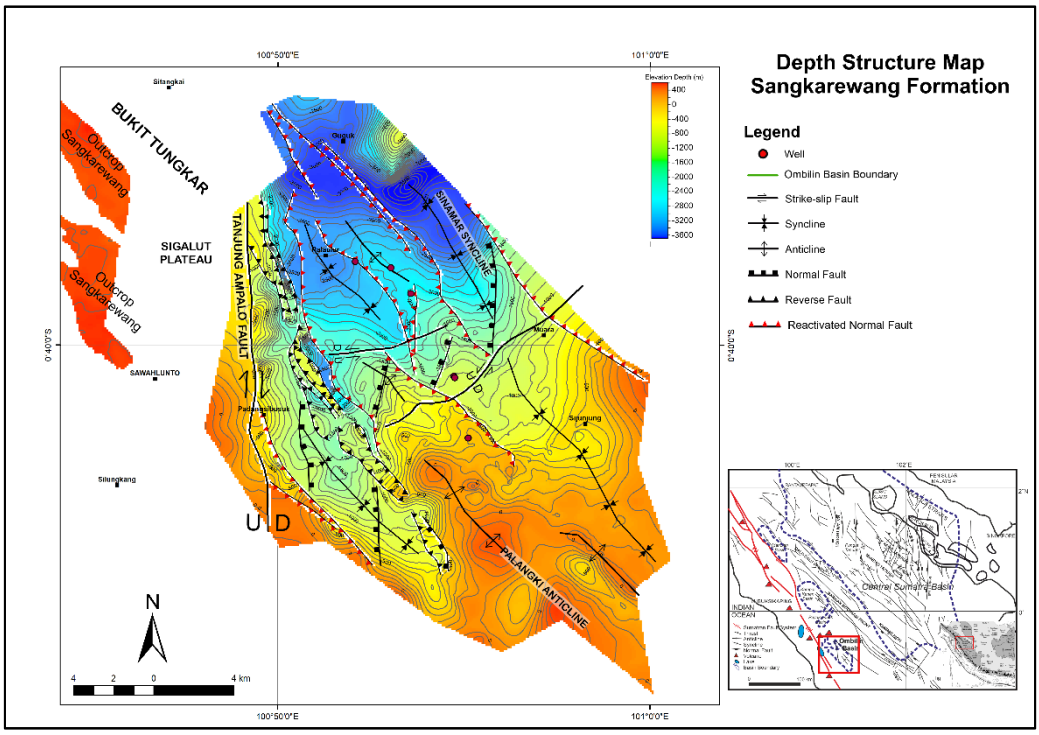

Figure 23. The depth structure of Top Sangkarewang Formation. The structure is dominated by the N-S and NW-SE trend faults. The deepest depocenter is near the Guguk area on the south of Takung Fault.

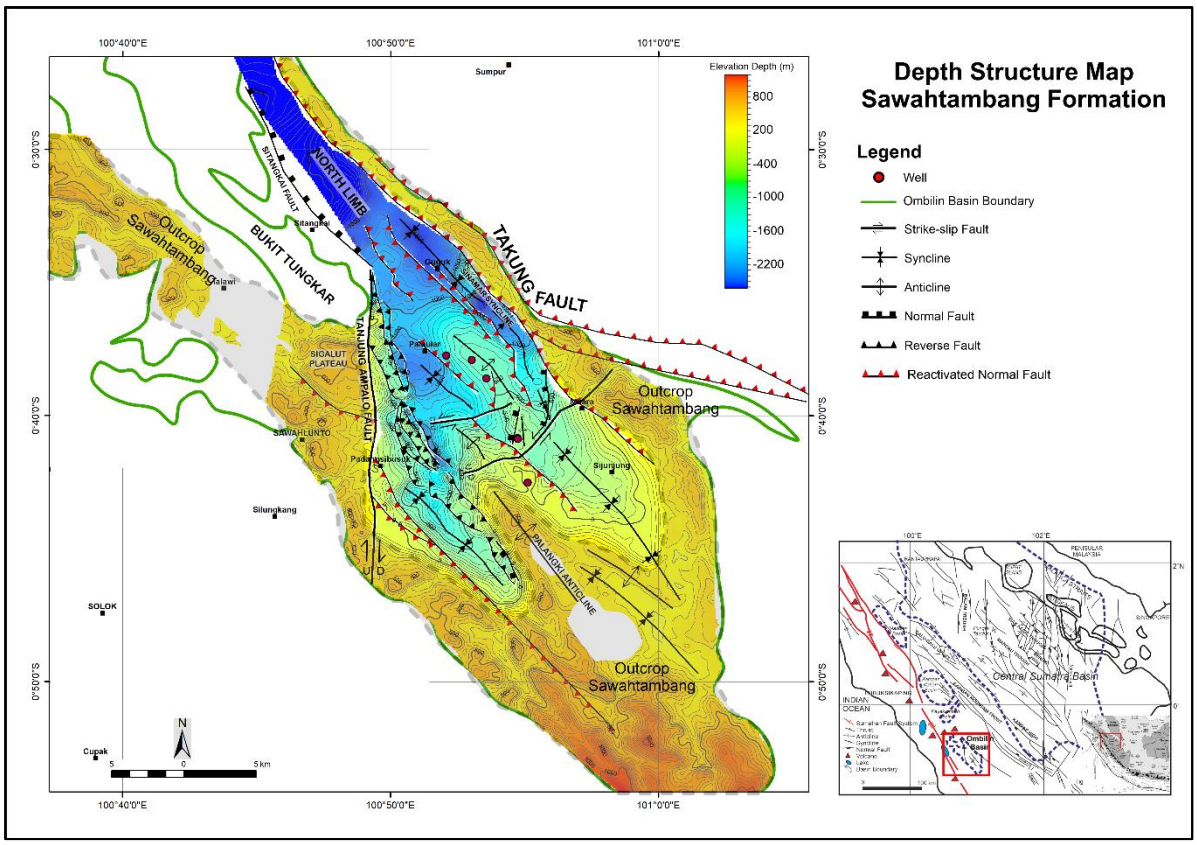

Figure 24. The depth structure of Top Sawahtambang Formation that has been combined with the outcrop data (the area inside the dashed line) from the surface geology map. The structure is dominated by the NW-SE trend faults. Because the rifting started to stop at the end of Sawahtambang Formation, the N-S structure is barely seen in this map. The deepest depocenter is near the Guguk area on the south of Takung Fault.

5. Discussion

The existence of several gentle reverse faults that are dipping to the northeast (fault L1 to L4 in Figure 18Figure 19Figure 20) may lead to misleading interpretation. If we consider the geometry of the Ombilin Basin from the NE-SW seismic section (Figure 18 & Figure 19) and make a tectonic interpretation from the perspective of the current subduction established since Mid-Eocene (ca. 45 Ma Hall, 2012), may be tempting to interpret the basin was formed under a compressional setting as a piggyback basin. However, prior in the Early Paleogene, the extensional phase in Sundaland including the Sumatra already resulted in the development of horsts and grabens (Barber et al., 2005), and is in agreement with the earlier -origin and structuration of the Ombilin Basin.

5.1. Rifting model of the Ombilin Basin

The Early Paleogene E-W extensional stresses (Hall, 2009) resulted in the graben development in the Ombilin Basin. The rifting initiation was controlled by the N-S normal faults as the master fault and the NW-SE of inherited basement structures as the transfer fault (Figure 25). Because of these controlling faults, the segmented E-W rifting occurred resulted in the development of the N-S oriented grabens. At this phase, the Paleocene-Early Eocene alluvial fan of the Brani Formation from the local horst blocks and lacustrine shale of the Sangkarewang Formation were deposited. Different subsidence rates of each basin floor causing the variation of basin depth. It is evidenced by the most prominent subsided area in the Sinamar Sub-basin is not in the basin center but rather in the northern

area (Figure 25) near the Guguk area (Figure 21). The N-S oriented Tanjung Ampalo Fault, presumably a normal fault, accommodated the deepening of the grabens in the Sinamar sub-basin.

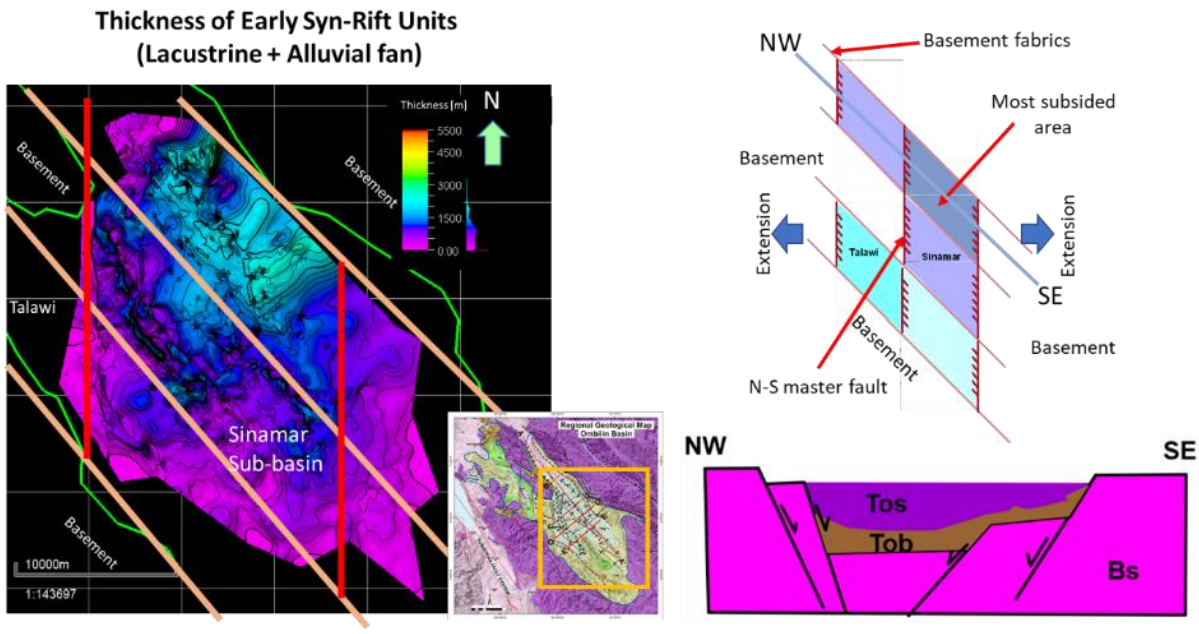

Figure 25. The thickness map of the early rift units and the rifting mechanism. The early syn-rift of the Ombilin Basin in the Paleocene-Early Eocene and the deposition of Brani Formation (Tob) interfingers with Sangkarewang Formation (Tos) during the early Paleogene extension. The rifting was accommodated by the N-S trend structure (red line) that acted as the master fault and the NW-SE trend inherited basement fabrics (pink line) as transfer fault creating the N-S oriented. The thickest sediment and deepest depocenter of the Sinamar Sub-basin are located in the northern center area. This is due to the segmented rifting mechanism in the Ombilin Basin.

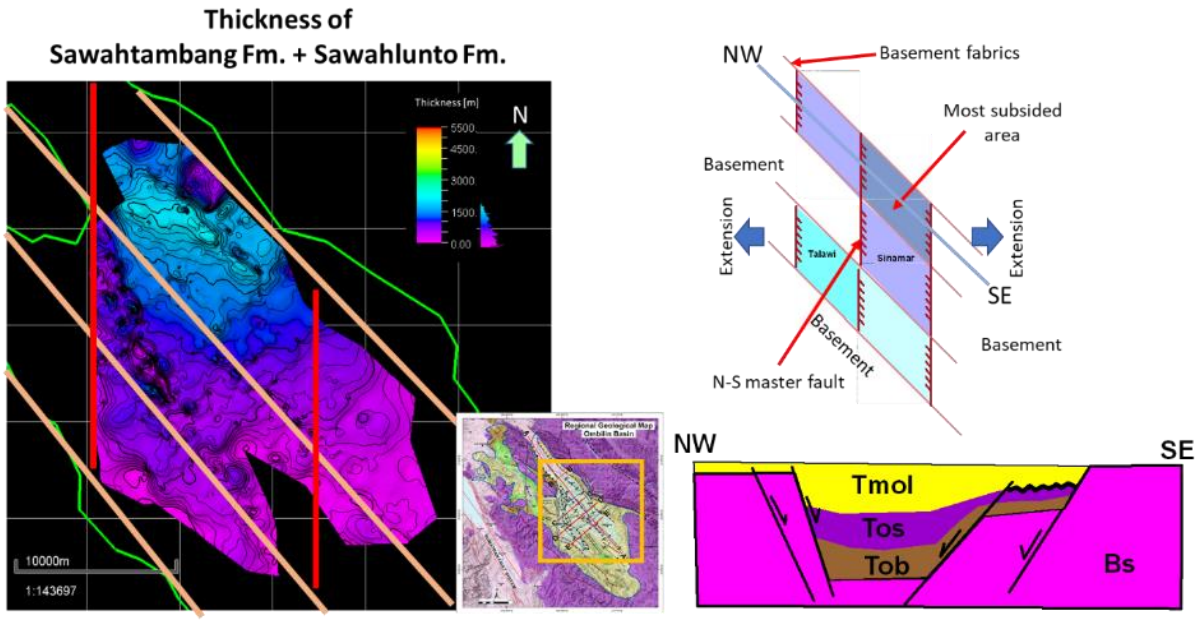

Figure 26. The thickness map of the late syn-rift units (the Late Eocene Sawahlunto Formation and the Oligocene Sawahtambang Formation (both represented by Tmol)). A similar rifting mechanism model still affecting the development of the basin in the Late Eocene-Late Oligocene. This phase is marked by the erosion of the early sin-rift units in the SE area of the basin edge while the deposition of the late syn-rift units.

The rifting continued in the Late Eocene to Late Oligocene with a similar mechanism. The change of global sea level by regression in the Eocene-Oligocene creates regional unconformity in the Sumatra

(c. 40 Ma in Barber et al., (2005)). In the Ombilin Basin, the regional unconformity is marked by the angular unconformity in the southeastern part (Figure 12) in which part of the Brani and Sangkarewang formations eroded. The rapid changing of the depositional environment in the Ombilin Basin from lacustrine to meandering river environment created a euxinic condition allowing the sedimentation of coal-bearing sediments of the Late Eocene Sawahlunto Formation in the fluvio-deltaic environment and the Oligocene Sawahtambang formations in the braided river system, respectively (Figure 26).

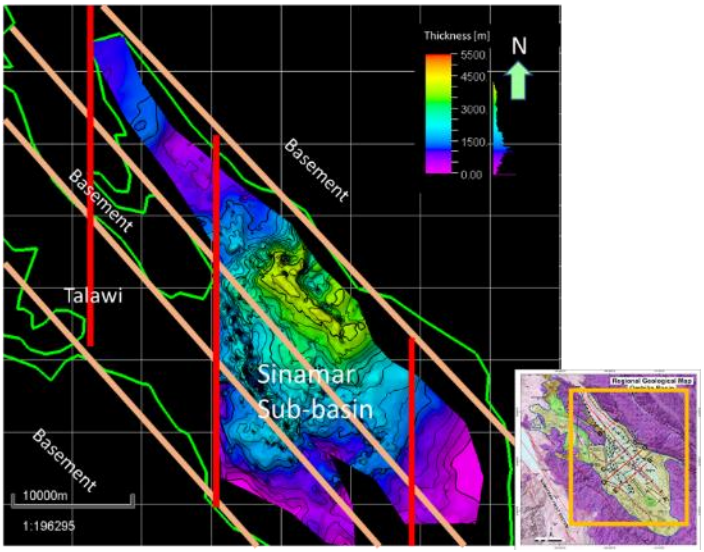

Figure 27. The total thickness of the syn-rift sediments. The thickest sediment around 4500 m in the northern center area has been deposited from the Early Cenozoic to the Late Oligocene.

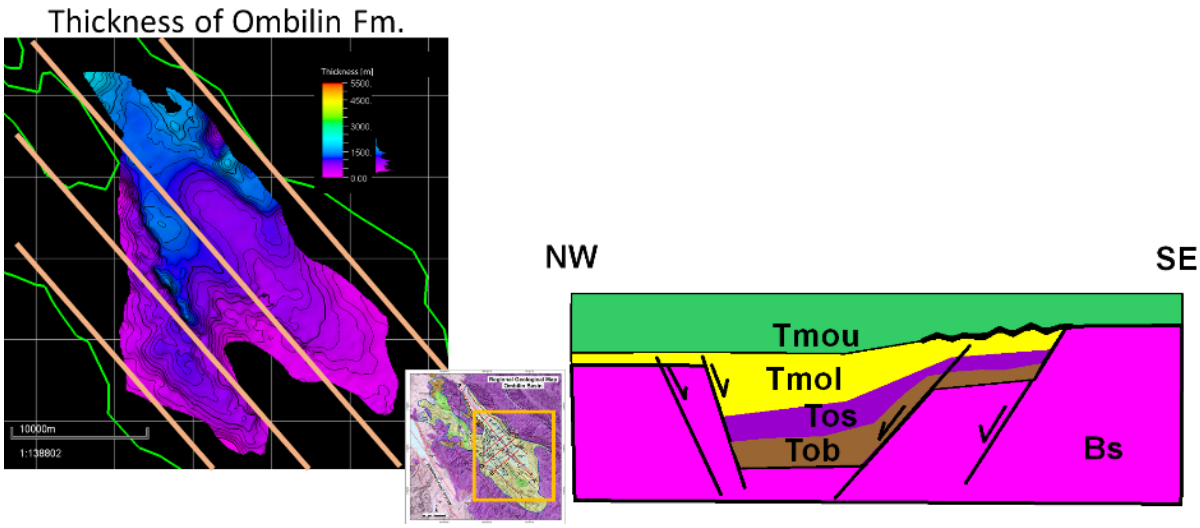

Figure 28. The present-day thickness map of the Early Miocene Ombilin Formation (Tmou). The thickest preserved post-rift unit is deposited in the North Limb area (ca. 1500 m thick). The preserved thickness of the Ombilin formation that is thinner in the SE area is subjected to the extensive erosion following the basin inversion since the Mid-Miocene.

At the end of the Sawahtambang deposition (Late Oligocene), the rifting ceased resulting in deposition further to the northwest area to fill up the basin (Figure 26). The cessation of rifting is evidenced by the fault L6 (Figure 15), which does not extend beyond the top of the Sawahtambang Formation.

This interpretation implies that rifting ceased much later than postulated by Barber et al. (2005), which assumes that the Sawahlunto and Sawahtambang formations were deposited during the regional sag (Post-rift).

At the end of the syn-rift phase, a total of 4500m preserved sediments were deposited from the early Cenozoic to the Late Oligocene (Figure 27) in the segmented rifting mechanism that was controlled by the N-S structures and NW-SE basement fabrics.

The change of the tectonic regime to the regional sagging in the latest Oligocene yielded the erosion of the Sawahtambang formation at the basin edge in the southeast area (Figure 28. The present-day thickness map of the Early Miocene Ombilin Formation (Tmou).. This erosion is detected from a clear angular unconformity (Figure 12) and most likely occurred due to basin subsidence from the thermal relaxation in the sagging phase. Subsequently, the marine shale sediment of the Ombilin Formation was deposited in the Early Miocene as a post-rift deposit.

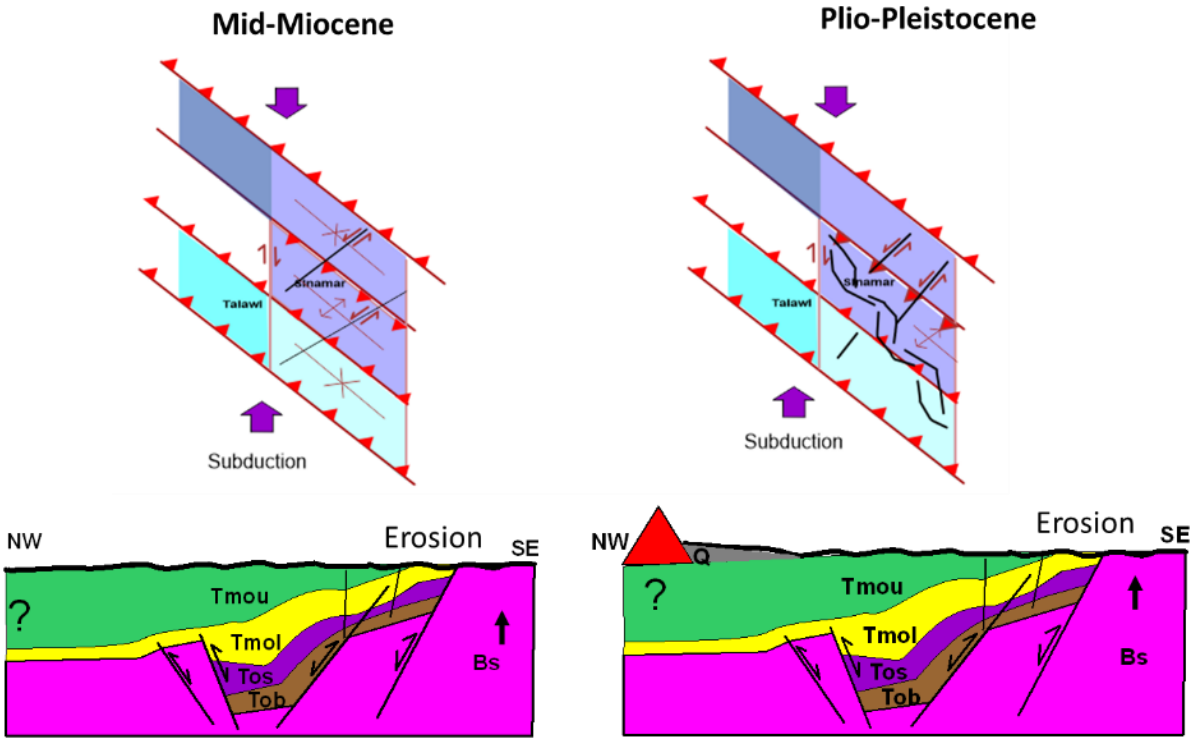

Figure 29. The basin inversion that occurred in the Mid-Miocene yield the rejuvenation of the early N-S fault and the NW-SE inherited basement fabrics to become the reverse faulting and some of the N-S faults became strike-slip faults. This is together with the development of the back-thrusting as a conjugate fault and the NW- SE trend folds, which can be seen from the NE-SW seismic profile (Figure 18, Figure 19, Figure 20). Continuous compressional setting in the Plio-Pleistocene tectonic phase induced the development of several strike-slip faults, including the NW-SE anastomosing fault pattern and the NE-SW sinistral strike-slip.

The compression related to the subduction in the Mid-Miocene yielded the initiation of the Barisan Mountain and the generation of the dextral Sumatran Fault System. This induced the basin inversion in the Ombilin Basin, which rejuvenated the early N-S fault and the NW-SE inherited basement fabrics in reverse faults and some of the N-S faults became strike-slip faults (Figure 29). This was coincident with the development of the conjugate southwest dipping back-thrusts and NW- SE trend folds as well as the development of the petroleum system in this basin (Figure 18). In addition, the flower structure crossing the youngest strata (Figure 19) was developed culminating during Plio-Pleistocene inversion (Figure 29).

Extensive erosion following the uplift affected the Ombilin Basin since the Mid-Miocene. From the surface geological map (Figure 11) it is seen that the youngest sediment of the Early Miocene Ombilin Formation only preserved in the Sinamar. Meanwhile, the older strata of the Paleocene- Eocene Brani and Sangkarewang formations are mainly exposed in the Talawi area, only at some locations the Sangkarewang Formation is exposed in the southern part of Sinamar. From the geological map, it is evident that different rates of erosion affected the Ombilin Basin, in agreement with the structural style of basin inversion evidenced from the subsurface interpretation.

5.2. Comparison to other Tertiary basins in Sumatra

The structural style of rifting observed in the Ombilin Basin bears in our view a close correspondence to structural style observed in sub-basins in the Central Sumatra Basin located to the northeast of the Ombilin Basin (Figure 30) as described by Moulds (1989) for the Bengkalis Graben. Prior to the extension in the Early Paleogene, the Sumatra island composed of NW-SE basement fabrics (Figure 30A). When the extension occurred, the rifting was facilitated by the N-S trending fractures that crossed the shortest route through the NW-SE lineaments of basement weakness (Figure 30B). It allows the development of the N-S oriented graben (Figure 30C) and several side grabens as a result of continuous extension (Figure 30D).

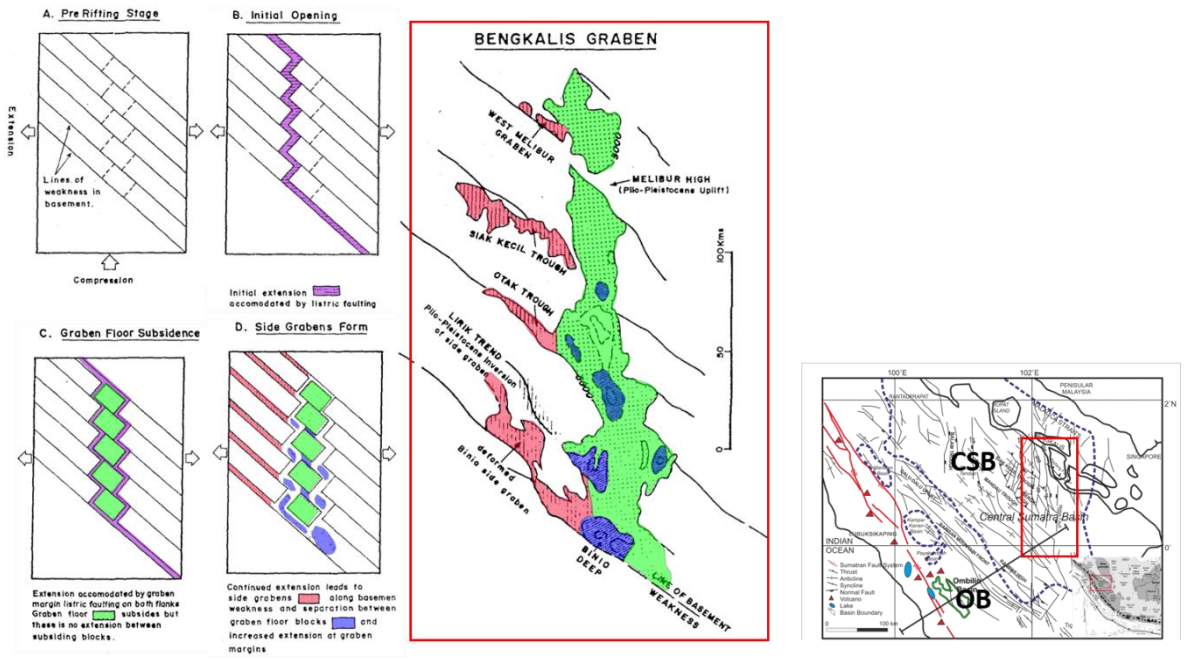

Figure 30. The model development of the Bengkalis graben by Moulds (1989).

The Moulds' model explanation fits with the Ombilin Basin. The Ombilin Basin has N-S oriented faults that acted as master faults when the rifting occurred while the side grabens (preferable the Talawi Sub-basin) were developed as a result of segmented rifting. This is also supported by the vitrinite reflectance analysis that suggests the Talawi Sub-basin did not subside to the same depth as the Sinamar Sub-basin (Moss & Carter, 1996). Thus, reminiscing that in the present day the older strata are mainly exposed in the Talawi Sub-basin and because this sub-basin is closer to the active Sumatran Fault System, the Talawi is more uplifted and experienced more severe erosion than the Sinamar. The application of Moulds model on the Ombilin Basin can be seen in Figure 31.

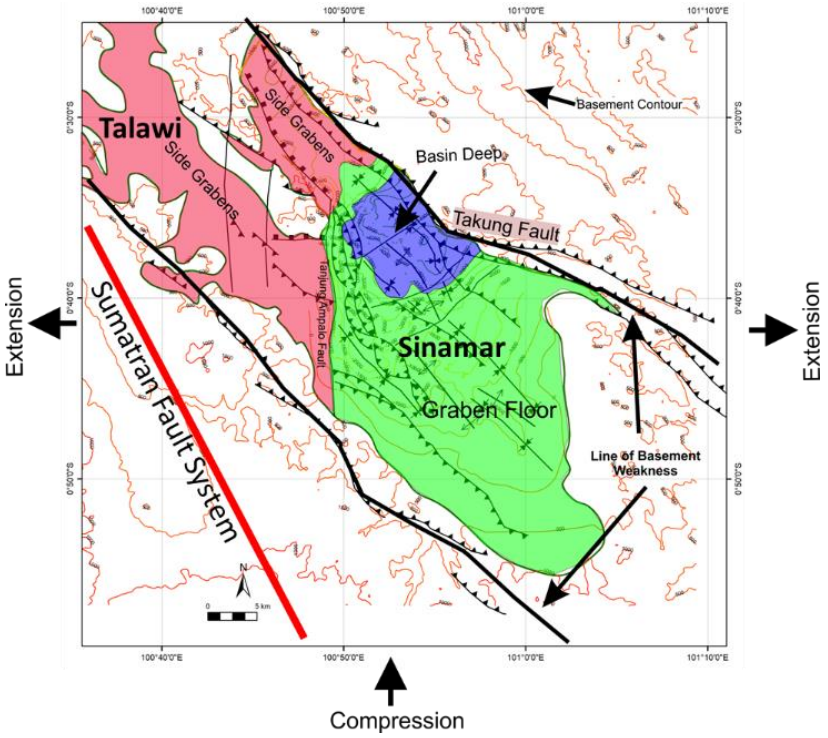

Figure 31. The Moulds (1989) model on the Ombilin Basin. The N-S oriented faults that are bounded by the NW-SE inherited basement fabrics acted as the master fault when the rifting occurred, and the side grabens developed as a result of continuous segmented rifting.

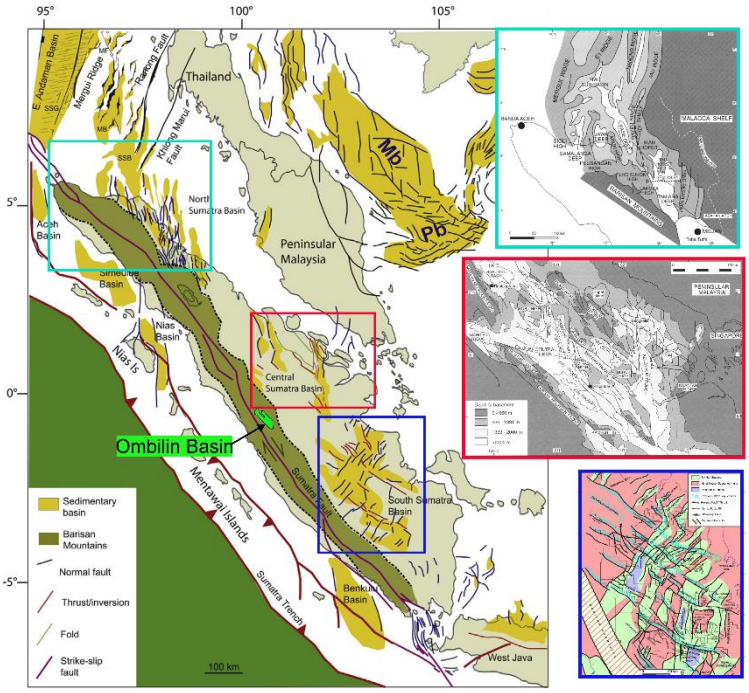

Figure 32. The figure showing the present geometry and trend of the basin depocenters in Sumatra (modified from Pubellier & Morley, 2014) *with the inset of North Sumatra Basin (cyan box) from* Barber et al. (2005)*, the Central Sumatra Basin (red box) from* Heidrick & Aulia (1993)*, and the South Sumatra Basin (blue box) from* Ginger & Fielding (2005)*.*

The other much larger Tertiary basins, such as the North Sumatra Basin, the Central Sumatra Basin, and the South Sumatra Basin also consist of several segmented N-S oriented depocenters (Figure 32). This is an indication that these basins experience a similar extensional mechanism.

The geometry of the depocenter of these three basins (North Sumatra Basin, Central Sumatra Basin, South Sumatra Basin) slightly perpendicular to the trench trend. Therefore, the mechanism of the rifting process is presumably not as simple as it seems, but rather more complex process.

The N-S oriented graben is also found in the western Sundaland around Southern-Thai Peninsula (Figure 32). Sautter et al. (2015) suggested that the rifting initiation in the Eocene in this area was accommodated by large crustal-scale low-angle normal faults, which reactivated the basement structures by right-lateral transpressional tectonics. Meanwhile, in the later work by Sautter et al. (2019), they explained that the extension in Sundaland was driven by the underplating of the Greater India's excess topography to the western Sundaland during the northward migration of Indian Plate in the early Paleogene (ca. 45 Ma). This resulted in uplift, thermal anomalies, and extensional exhumation then followed by subsidence due to gravitational collapse.

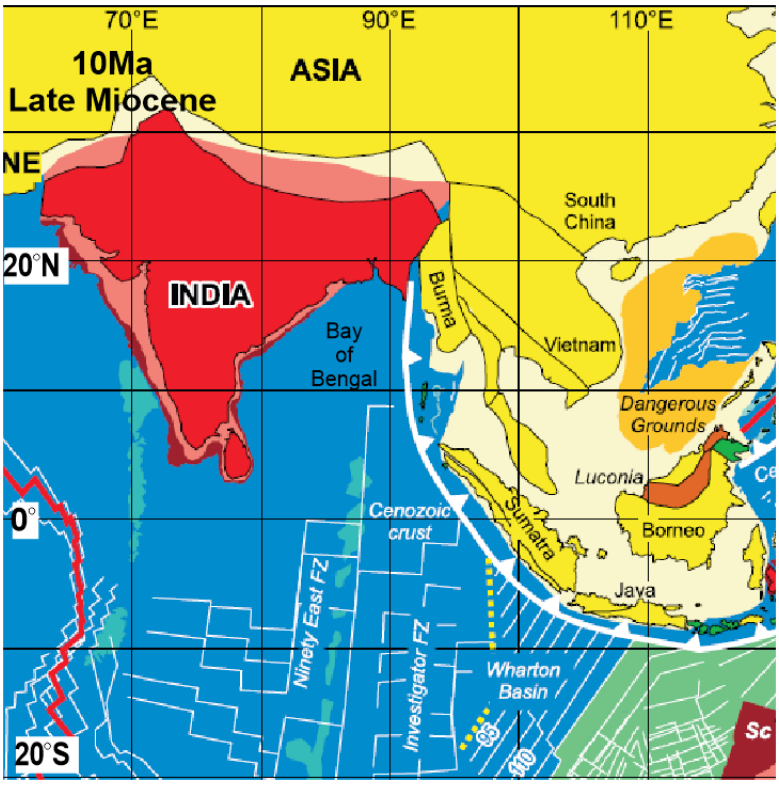

*Figure 33. Map to show the position of Ninety East Ridge (*modified from Hall, 2012)

The northward migration of the Indian plate in the Late Cretaceous was accommodated by a lateral inactive spreading ridge called the Ninety East Ridge (Figure 33), which stretches from the Bay of Bengal to the south within the Indian Ocean, far to the west of Sumatra. Therefore, the mechanism of orogenic collapse proposed by Sautter et al. (2015, 2019) probably only applied for the basin in the western Sundaland at the area of the nearby orogenic belt or on the north of Sumatra island. Meanwhile, if the basin development was influenced by a slab rollback along the Sumatra-Java margin, the basin depocenter orientation would likely be parallel to the subduction trend.

Figure 31 depicts the geometry of the Bengkalis Trough, which is narrow in the north and wider in the south (Figure 30). This can be explained by the oroclinal bending model by Hutchison (1994). Based on paleomagnetic data, He suggested that the anticlockwise rotation of India (Greater India in Hall, 2012) while collided to Eurasia during the early Paleogene induced the clockwise rotation of the NW-SE trending Thai-Malay Peninsular into their present position. This also coincides with the

anticlockwise rotation of SW Borneo (Figure 34). The oroclinal bending induced a compressional setting in the inner part while pull-apart in the outer part of orocline.

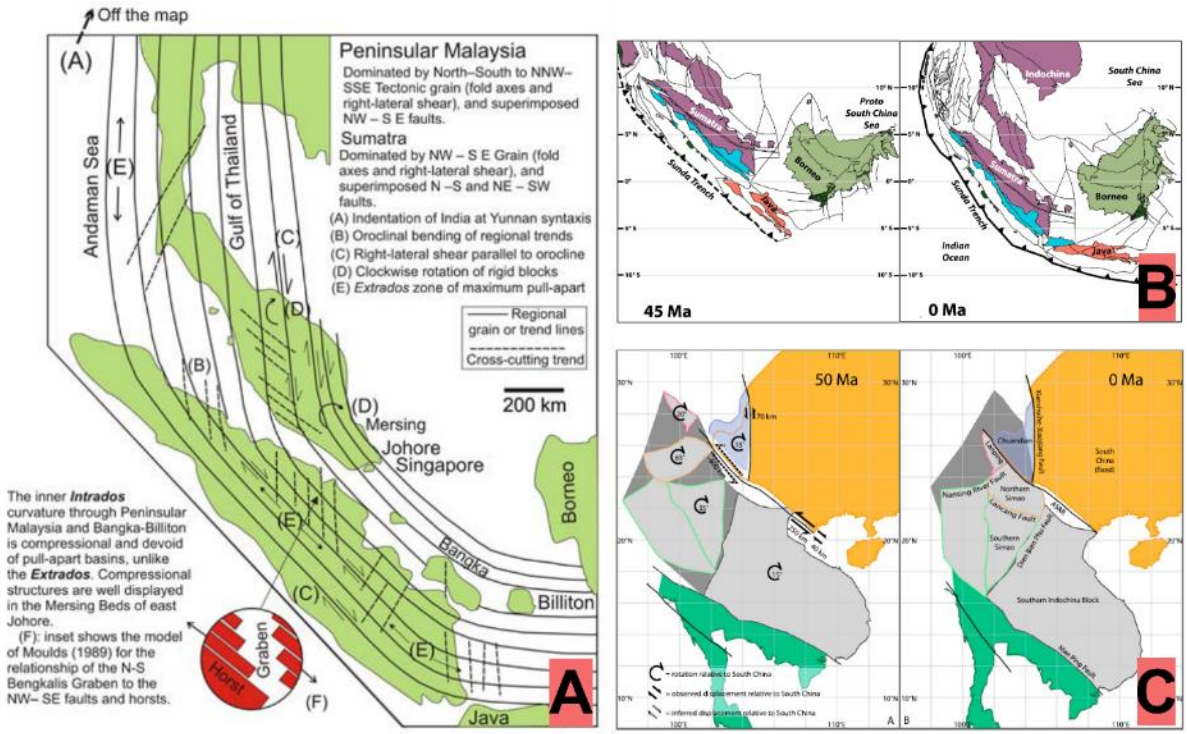

Figure 34. (A) Oroclinal bending model of Hutchison (1994*) in* Hutchison (2014)*. The regional solid lines are the strike lines of Triassic strata. (B) The inset to show the anticlockwise rotation of Borneo by* Advokaat, Marshall, et al. (2018)*. (C) The inset to show the clockwise rotation of Thai-Malay Peninsular as an implication of IndoChina rotation by* (Li et al., 2017)*.*

The argument about a pull-apart setting is questionable. First, he did not consider the timing of Sumatran Fault Systems which was initiated in the Mid-Miocene. Second, there is no evidence about the occurrence of mega strike-slip fault that active during the Early Cenozoic. Therefore, further studies are needed to explain the more concrete rifting mechanism in Sumatra.

6. Conclusion

The Ombilin Basin is an ideal analogue to study the rifting and subsequent inversion mechanism of the early Tertiary Basins in Sumatra, because of its excellent sediment and structuration record and data availability for stratigraphic and structural interpretation, from wells, seismic, DEM, and outcrop data.

Building from detailed seismic interpretation and structural analysis, this study interprets the Ombilin Basin as a rift basin originally formed in a half-graben geometry that developed during the extensional phase in the Early Paleogene. The geometrical style of rifting and the spatial and temporal variation in rates of subsidence are due to a segmented rifting mechanism that was controlled by the N-S normal faults as master faults and NW-SE inherited basement structures as the transfer fault. Therefore, the Ombilin basin is not a classic extensional basin that is caused by the subduction rollback.

The NW-SE oriented structure of Takung Fault is the inherited basement fabrics that were reactivated as a reverse fault during the basin inversion since the Mid-Miocene together with the initiation of Barisan mountain and the dextral strike-slip of Sumatran fault system. Meanwhile, the N-S structure of Tanjung Ampalo is initially a normal fault that acted as the master fault during the rifting phase,

which later rejuvenated as a dextral strike-slip in the later tectonic phase (Plio-Pleistocene). This was together with the development of other strike-slip components in the Ombilin Basin.

Based on the observations and evidence presented in this paper, we dismiss the hypothesis that the Ombilin Basin originated as a pull-apart basin since strike-slip structures were mainly activated during later time cross-cutting the youngest strata. In our view, the Ombilin basin structuration follows the conceptual model of the Moulds (1989) and is in agreement with large scale oroclinal bending by Hutchison (1994), which jointly can explain that the initiation of basins all over Sumatra was developed as a result of the local extension marked by several partitions of depocenters rather than a one geometrically unified rifting structure. In other words, our evidence suggests that the Ombilin Basin and Central Sumatra Basin including other Sumatran Tertiary basins were developed under similar rifting systems prior to the emergent of the Barisan Mountain. Therefore, it dismisses the conceptual model of Barber et al. (2005) that the Ombilin basin and Central Sumatra Basin were originally one unified basin that later separated during the Barisan Orogeny in the Late Miocene.

7. Recommendation for further studies

1. The updated tectonostratigraphic based on the proposed model
2. The kinematic study of the NW-SE trending anastomosing fault
3. The re-evaluation of the petroleum play system

Acknowledgment

I would like to thank LPDP (Indonesia Endowment Fund for Education) for fully funding my master's study at Utrecht University. I also extend my appreciation to PT. Rizki Bukit Barisan Energi who kindly gave me access to the data (seismic and well marker) to perform my MSc. Research.

First and foremost, I would also like to extend my deepest gratitude to all my supervisors. Jan-Diederik van Wees for his insightful suggestion and expertise so this thesis can be brought into a higher level. Jeroen Smit, his wide perspective and systematic approach encourages my enthusiasm to enhance my critical thinking in the field of tectonics. Lukman Sutrisno, his generous assistance and discussion about tectonic in Sumatra was greatly appreciated. Without their invaluable guidance and constructive suggestions, this research would have never been accomplished.

Most importantly, none of this could have happened without the support of my family - my parents for their moral and emotional blessing throughout my life. My wife, Avie R. Puteri who extends her love, prayers, and believes to keep me going to complete this study.

References

Abdullah, A., Akhir, J. M., & Abdullah, I. (2010). Automatic mapping of lineaments using shaded relief images derived from digital elevation model (DEMs) in the Maran - Sungi Lembing area, Malaysia. *Electronic Journal of Geotechnical Engineering*, *15 J*, 949–957.

Advokaat, E. L., Bongers, M. L. M., Rudyawan, A., BouDagher-Fadel, M. K., Langereis, C. G., & van Hinsbergen, D. J. J. (2018). Early Cretaceous origin of the Woyla Arc (Sumatra, Indonesia) on the Australian plate. *Earth and Planetary Science Letters*, *498*, 348–361. https://doi.org/10.1016/j.epsl.2018.07.001

Advokaat, E. L., Marshall, N. T., Li, S., Spakman, W., Krijgsman, W., & van Hinsbergen, D. J. J. (2018). Cenozoic Rotation History of Borneo and Sundaland, SE Asia Revealed by Paleomagnetism, Seismic Tomography, and Kinematic Reconstruction. *Tectonics*, *37*(8), 2486–2512. https://doi.org/10.1029/2018TC005010

Barber, A. J., Crow, M. J., Milsom, J. S., & (eds). (2005). *Sumatra: Geology, Resources and Tectonic Evolution*. Geological Society, London, Memoirs, 31.

Clark, C. D., & Wilson, C. (1994). Spatial analysis of lineaments. *Computers and Geosciences*, *20*, 1237–1258. https://doi.org/10.1016/0098-3004(94)90073-6

Digital Elevation Model (DEM) of Indonesia. (n.d.). Geospatial Information Agency of Indonesia (available on https://big.go.id).

Dooley, T. P., & Schreurs, G. (2012). Analogue modelling of intraplate strike-slip tectonics: A review and new experimental results. In *Tectonophysics* (Vols. 574–575, pp. 1–71). https://doi.org/10.1016/j.tecto.2012.05.030

Fletcher, G., & Yarmanto. (1993). *Ombilin Basin Field Guide Book* (pp. 1–59). Indonesian Petroleum Association, Post convention field trip.

Francis, A. (2018a). *A Simple Guide to Seismic Depth Conversion I; Part I: A simple guide to the parameters involved in seismic depth conversion - a complex but important subject in geophysical seismic processing*. Geoexpro Vol. 15 No.2. https://www.geoexpro.com/articles/2018/05/a-simple-guide-to-seismic-depth-conversion-i

Francis, A. (2018b). *A Simple Guide to Seismic Depth Conversion II; Part II: A step by step guide to learning and mastering depth conversion in geophysics*. Geoexpro Vol. 15 No.3. https://www.geoexpro.com/articles/2018/08/a-simple-guide-to-seismic-depth-conversion-ii

Ginger, D., & Fielding, K. (2005). The petroleum systems and future potential of the South Sumatra basin. *Proc. Indonesian Petroleum Association 30th Annual Convention*.

Habrianta, L., Matthew, G., Akhrurozi, F., Auliansyah, D., & Andhika, I. P. (2018). A Semi-Regional Play Analysis of the South Sumatra, Ombilin Basin to Understand the Tectono-Stratigraphic Framework and Identification of Potential Exploration Opportunities. *Proc. Indonesian Petroleum Association 42nd Annual Convention*.

Hall, R. (2009). Hydrocarbon basins in SE Asia: Understanding why they are there. *Petroleum Geoscience*, *15*(2), 131–146. https://doi.org/10.1144/1354-079309-830

Hall, R. (2012). Late Jurassic-Cenozoic reconstructions of the Indonesian region and the Indian Ocean. *Tectonophysics*, *570–571*, 1–41. https://doi.org/10.1016/j.tecto.2012.04.021

Hall, R., & Morley, C. K. (2004). Sundaland basins. In P. Clift, W. Kuhnt, P. Wang, & D.Hayes (Eds.), *Continent–Ocean Interactions Within East Asian Marginal Seas* (pp. 55–85). American Geophysical Union. https://doi.org/10.1029/149GM04

Heidrick, T. L., & Aulia, K. (1993). A Structural and Tectonic Model of the Coastal Plains Block, Central Sumatra Basin, Indonesia. *Proc. Indonesian Petroleum Association 22nd Annual Convention*, 285–317.

Howells, C. (1997). Tertiary response to oblique subduction and indentation in Sumatra, Indonesia: new ideas for hydrocarbon exploration. *Geological Society Special Publication*, *126*(Petroleum Geology of Southeast Asia), 365–374. https://doi.org/10.1144/GSL.SP.1997.126.01.22

Husein, S., Barianto, D. H., Novian, M. I., Putra, A. F., Saputra, R., Rusdiyantara, M. A., & Nugroho, W. (2018). Perspektif baru dalam evolusi cekungan ombilin sumatera barat. *Proceeding Seminar Nasional Kebumian Ke-11 UGM*, *September*.

Hutchison, C. S. (1994). Gondwana and Cathaysian blocks, palaeotethys sutures and cenozoic tectonics in South-east Asia. *Geologische Rundschau*, *83*(2), 388–405. https://doi.org/10.1007/BF00210553

Hutchison, C. S. (2014). Tectonic evolution of Southeast Asia. *Bulletin of the Geological Society of Malaysia*, *60*, 1–18.

Koesoemadinata, R. P., & Matasak, T. (1981). Stratigraphy and sedimentation: Ombilin Basin, Central Sumatra (West Sumatra Province). *Proc. Indonesian Petroleum Association 10th Annual Convention*, 217–250. https://doi.org/10.29118/ipa.343.217.249

Koning, T. (1985). Petroleum geology of the Ombilin intermontane basin, West Sumatra. *Proc. Indonesian Petroleum Association 14th Annual Convention*, 117–137.

Li, S., Advokaat, E. L., van Hinsbergen, D. J. J., Koymans, M., Deng, C., & Zhu, R. (2017). Paleomagnetic constraints on the Mesozoic-Cenozoic paleolatitudinal and rotational history of Indochina and South China: Review and updated kinematic reconstruction. *Earth-Science Reviews*, *171*(June 2017), 58–77. https://doi.org/10.1016/j.earscirev.2017.05.007

McClay, K., & Bonora, M. (2001). Analog models of restraining stepovers in strike-slip fault systems. *AAPG Bulletin*, *85*(2), 233–260. https://doi.org/10.1306/8626c7ad-173b-11d7-8645000102c1865d

Metcalfe, I. (1996). *Pre-Cretaceous evolution of SE Asian terranes*.

Metcalfe, I. (2013). Gondwana dispersion and Asian accretion: Tectonic and palaeogeographic evolution of eastern Tethys. *Journal of Asian Earth Sciences*, *66*, 1–33. https://doi.org/10.1016/j.jseaes.2012.12.020

Morley, C. K. (2002). A tectonic model for the Tertiary evolution of strike-slip faults and rift basins in SE Asia. *Tectonophysics*, *347*(4), 189–215. https://doi.org/10.1016/S0040-1951(02)00061-6

Moss, S. J., & Carter, A. (1996). Thermal histories of Tertiary sediments in western central Sumatra, Indonesia. *Journal of Southeast Asian Earth Sciences*, *14*(5), 351–371. https://doi.org/10.1016/S0743-9547(96)00071-2

Moulds, P. J. (1989). Development of the Bengkalis Depression, Central Sumatra and Its subsequent Deformation - a Model for Other Sumatran Grabens? *Proc. Indonesian Petroleum Association 18th Annual Convention*, 217–244.

Murray, A. M., Zaim, Y., Rizal, Y., Aswan, Y., Gunnell, G. F., & Ciochon, R. L. (2015). A fossil gourami (Teleostei, Anabantoidei) from probable Eocene deposits of the Ombilin Basin, Sumatra, Indonesia. *Journal of Vertebrate Paleontology*, *35*(2), 37–41. https://doi.org/10.1080/02724634.2014.906444

Musper, K. A. F. R. (1930). Beknopt verslag over de uitkomsten vannieuwe geologische

onderzoekingen in de Padangsche Bovenlanden, Jaarb. Mijnw . Ned. Indie , vold. LVIII, 1929 Verhandlingen ,303- 313. *Barber, A. J., Crow, M. J., Milsom, J. S., & (Eds). (2005). Sumatra: Geology, Resources and Tectonic Evolution. Geological Society, London, Memoirs, 31.*

Noeradi, D., Djuhaeni, & Simanjuntak, B. (2005). Rift play in Ombilin Basin outcrop, West Sumatra. *Proc. Indonesian Petroleum Association 30th Annual Convention*, *1*, 39–51.

Pubellier, M., & Morley, C. K. (2014). The basins of Sundaland (SE Asia): Evolution and boundary conditions. *Marine and Petroleum Geology*, *58*(PB), 555–578. https://doi.org/10.1016/j.marpetgeo.2013.11.019

Pulunggono, A., & Cameron, N. . (1984). Sumatran Microplates, Their Characteristics and Their Role in The Evolution of the Central and South Sumatra Basins. *Proc. Indonesian Petroleum Association 13th Annual Convention*.

Sapiie, B., Aprianyah, D., Tureno, E. Y., & Manaf, N. A. (2017). A New Approach in Exploring a Basement-Fractured Reservoir in the SUmatra Back-arc basin. *Proc. Indonesian Petroleum Association 41st Annual Convention*.

Sautter, B., Pubellier, M., Králiková Schlögl, S., Matenco, L., Andriessen, P., & Mathew, M. (2019). Exhumation of west Sundaland: A record of the path of India? *Earth-Science Reviews*. https://doi.org/10.1016/j.earscirev.2019.102933

Sautter, B., Pubellier, M., & Menier, D. (2015). Late Mesozoic tectonics of the Southern-Thai Peninsula : from transpression to basins opening. *Geophysical Research Abstracts*, *December 2016*, 16–17.

Silitonga, P. H., & Kastowo. (1975). *Geological Map of the Solok Quadrangle (0815), Sumatra. Scale 1:250 000*. Geological Survey of Indonesia, Ministry of Mines, Bandung.

Silitonga, P. H., & Kastowo. (1995). *Geological Map of the Solok Quadrangle, Sumatera (Quadrangle 0815) Scale 1:250,000. 2nd Edition*. Geological Research and Development Centre Bandiung. Edition 2.

Situmorang, B., Yulihanto, B., Guntur, A., Himawan, R., & Jacob, T. G. (1991). Structural development of the Ombilin Basin West Sumatra. *Proc. Indonesian Petroleum Association 20th Annual Convention*, 1–15.

Sutrisno et al., L. (n.d.). *Tectonic control of Inherited Basement Structures on the Sumatran Fault System and Volcanic Arc, Indonesia. Manuscript in preparation.*

Van Bemmelen, R. W. (1949). *The Geology of Indonesia*. Martinus Nijhoff, The Hague, Netherlands.

Zonneveld, J. P., Zaim, Y., Rizal, Y., Ciochon, R. L., Bettis, E. A., Aswan, & Gunnell, G. F. (2012). Ichnological constraints on the depositional environment of the Sawahlunto Formation, Kandi, northwest Ombilin Basin, west Sumatra, Indonesia. *Journal of Asian Earth Sciences*, *45*, 106–113. https://doi.org/10.1016/j.jseaes.2011.06.017

Appendix

1. Stratigraphic Setting

It is beyond the scope of this research to examine the stratigraphy of the Ombilin Basin. Therefore, to understand the lithological variation and sedimentation in the Ombilin Basin, the literature study was conducted.

1.1. Pre-tertiary Stratigraphy

Determining the Pre-Tertiary basement rocks in Sumatra as a whole is very complicated due to its poor bio-stratigraphic control, uncertain contact of each unit, and poorly exposed (Barber et al., 2005; Sapiie et al., 2017). However, the Pre-Tertiary rocks including the Permo-Carboniferous and Triassic limestones, slate, and phyllites as well as the Lassi Granite are well exposed in the Barisan Mountains, in particular surrounding the Ombilin Basin (Koning, 1985).

The underlying basement rocks of the Ombilin Basin comprise of meta-volcanic and meta-sediments of Silungkang Formation and Kuantan Formation, respectively. Fletcher & Yarmanto (1993) suggested these formations are part of the Mergui accretionary terrain, which later by Barber et al. (2005) are included in the West Sumatra Block. Those formations are manifested extensively on the surface around the edge as well as on the northern-central part of the basin together with a meta-sediment of Tuhur Formation and several granitic intrusion (Silitonga & Kastowo, 1975).

The Kuantan Formation lies on the east to the south of the Ombilin Basin. Pulunggono & Cameron (1984) considered this formation belongs to the Tapanuli Group, which also has similar lateral facies variation with the Bohorok, Alas, and Kluet Formations in the northern Sumatra. Silitonga & Kastowo (1975) differentiated Kuantan Formation into three different members: The Lower, the Phyllite and shale, and the Limestone Members. They are mainly comprised of low-grade metamorphic rocks: quartzite, phyllite/slate, and recrystallized limestone. The Limestone Member of this Kuantan Formation exposed by 2,5-5 km wide and 80 km long on the east of the Ombilin Basin, marked by the NW-SE orientation of distinct karst topography. This Limestone Member of Kuantan Formation comprises of white to grey massive recrystallized limestone, containing slate, phyllite, siliceous shale and quartzite, and grading into marble (Silitonga & Kastowo, 1975; Fletcher & Yarmanto, 1993). Musper (1929) predicted the Kuantan Formation age as the Lower or lower Upper Carboniferous while in Solok Quadrangle of Silitonga & Kastowo (1975) the age of this formation ranged from Lower Carboniferous to Mid-Permian.

The Silungkang and Tuhur Formations, which belong to the Peusangan Group, constitute the west of the Ombilin Basin (Pulunggono & Cameron, 1984; Barber et al., 2005). The lower Volcanic Member of Silungkang Formation, which expose around the Silungkang Village between the Sawahlunto and the Solok area, comprises of volcanic products, such as hornblende and augite andesite containing thin intercalations of shale, sandstone, limestone, and tuff (Silitonga & Kastowo, 1975; Koesoemadinata & Matasak, 1981; Barber et al., 2005). Meanwhile, the upper Limestone Member is composed of massive grey limestone that interbedded with shales, sandstones, and tuff (Silitonga & Kastowo, 1975. Fossil analysis from the fossiliferous rocks of the Limestone member indicates the Mid-Permian age (Barber et al., 2005).

The Tuhur Formation is classified into two members: the Limestone Member and the Slate and Shale Member. It is sparsely outcropped on the southwest of the Ombilin Basin and the east of Lake Singkarak. The Limestone Member composed of sandy limestone and conglomeratic limestone with thin intercalation of slate and shale. The fusulinids foraminifera of Permo-Triassic age was found from

the pebbles of conglomerates fragment (Musper, 1930). Meanwhile, the Slate and Shale Member is composed of grey to dark grey slate, brown cherts, and black shales together with thin greywacke sandstones (Silitonga & Kastowo, 1975; Barber et al., 2005). This formation is correlated to the Triassic sediments of Kualu Formation in the North Sumatra Basin (Barber et al., 2005).

The Lassi granite complex around the Pre-Tertiary rocks was suggested as the intrusion rock. However, it is difficult to determine the age of this intrusion rock due to a lot of inconsistency in dating. Koning (1985) estimated the age of this granite magmatism in the Ombilin Basin is ranging from Upper Jurassic to Cretaceous.

1.2. Tertiary Stratigraphy

The Tertiary Ombilin Basin fill is varied, it consists of littoral to inner-outer neritic marine sediments overlying the Pre-Tertiary Basement rocks. Six Tertiary sediments are covering the Ombilin Basin. These sediments from old to young are the Brani Formation, Sangkarewang Formation, the Sawahlunto Formation, the Sawahtambang Formation, the Ombilin Formation, and the Tuhur Formation, respectively.

1.2.1. Brani Formation

The Brani Formation composed of conglomerate and debris flow sediments called fanglomerate. On a large scale, these deposits exhibit convolute bedding and slumping structure (Barber et al., 2005). Characterized by a sequence of reddish-brown to purple polymict pebble- to cobble-conglomerates, muddy sand matrix, large variance of fragment sizes with and subangular to subrounded in shape, dense, and mostly non-bedded (Koesoemadinata & Matasak, 1981; Fletcher & Yarmanto, 1993). The color of the lithology indicates the existence of the rootlets or burrows within the Brani Formation (Fletcher & Yarmanto, 1993). Koesoemadinata & Matasak (1981) suggested these conglomerates are shortly transported due to their basement rock dependent pebble rock's type. Evidently, in the western part of the Ombilin Basin, they consist of volcanic and limestone materials, slates, and argillite pebbles whilst in the eastern part are dominated by granite pebbles. The measured section at locality near the Guguk area indicates fining upward sequence with some lenses of sandstones and claystones (Mukhayat in Koesoemadinata & Matasak (1981)).

The Brani Formation is exposed sparsely around the Ombilin Basin, especially in the northern center of the Ombilin Basin, the western part of the Talawi Sub-basin, and on the northwest between the Malintang Mountain and Marapi Volcano. The thickness is estimated ranges from 600 m and pinches out in various directions. Van Bemmelen (1949) assumed the conglomerates of Brani Formation are local deposits in the intermontane basins.

The Brani Formation unconformably overlies the Pre-Tertiary rocks or non-conformably on the plutonic rocks of the Pre-Tertiary units. It is also interfingering with Sangkarewang Formation. Due to the absence of fossil, the age of this unit is suggested similar to the Paleocene to Eocene Sangkarewang Formation (Koesoemadinata & Matasak, 1981).

The fanglomerate and rapid facies change along the basin margin indicate very high energy of sedimentation occurred within the Brani Formation, which correlates to the sedimentation process in the alluvial fan systems.

1.2.2. Sangkarewang Formation

The Sangkarewang Formation comprises brownish dark-grey to black finely laminated, papery calcareous shales. The sequence of the shales is fining upward, evidenced by the occurrence of graded-bedding sedimentary structure: coarse- to very fine-grained. Although calcareous, the Sangkarewang Formation contains carbonaceous material such as pyrite, mica, and plant-remains. The

Interbedded with thin grey to black calcareous sandstones with quartz to feldspar-bearing can be found near the Talawi area (outcrop measured section by Sulistio and Hartono in Koesoemadinata & Matasak (1981)). They determined the sandstones as the turbidite sediments at the beginning of the succession of Sangkarewang Formation when the sediments were transported from the steep slopes creating the slump structures, which typically found at the bottom of the sequence.

The Sangkarewang Formation is mostly exposed in the northwest area of the Talawi Sub-basin. It lies from the north of the Sawahlunto area to the east of Batu Sangkar in between the Brani Formation and Sawahtambang Formation.

Koesoemadinata & Matasak (1981) suggest the Sangkarewang Formation is laterally interfingering with the tongue of the Brani Formation and at some localities with the Sawahlunto Formation. It also unconformably overlies the Pre-Tertiary rocks.

Age determination of this formation is limited. The presence of fish fossils such as *Musperia Radiata*, *Scleropagus,* and *Anabantoidei* indicate Paleocene to Eocene in age (Musper, 1930; Murray et al., 2015). Koning (1985) suggested that the occurrence of macrofossils such as fresh-water fish and the anoxic mineral such as pyrite indicates this formation was deposited in the stable lacustrine environment.

The occurrence of lacustrine organic-rich shales provokes the hydrocarbon exploration in the Ombilin Basin. Furthermore, the total organic carbon (TOC) averaged 2.6 weight percent recorded from the exploration well of Sinamar No. 1 (Koning, 1985) yields the Sangkarewang Formation as a potential oil source rock.

1.2.3. Sawahlunto Formation

The Sawahlunto Formation characterized by the occurrence of the coal seams within its sediments. The formation composed of dense brown shales with conchoidal fractures, siltstones, quartz sandstones, and coals. The 126 m thick measured section at the Sawahlunto area by Siringo-ringo in Koesoemadinata & Matasak (1981) shows the shales typically carbonaceous and act as the underclay to the coal seam while the siltstones grading downwards into brown shale in the bottom of the succession. The coals are found interbedded with the grey siltstone and coaly clays. The sandstone layers are typically point-bar sequence with fining upward, current-ripple lamination with a sharp erosional base (Koesoemadinata & Matasak, 1981).

The Sawahlunto Formation is mainly exposed in the Talawi Sub-basin, on the northwest of Sawahlunto, where most coal mining activities are being conducted since the 1800s. The mining activities reveal the thickness of this formation ranging up to 300 meters. The interfingering with the Sangkarewang Formation yields conformable contact while also likely interfinger and locally unconformable with the overlying Sawahtambang Formation (Koesoemadinata & Matasak, 1981). The interface of the Sawahlunto-Sawahtambang Formation can be examined from the shift in vitrinite reflectance values from the oil exploration well, Sinamar No. 1 (Koning, 1985).

The Sawahlunto Formation is Eocene in age from spores and plant remains determination (detection of *Proxapertites Operculatus*). The occurrence of mentioned palynomorphs together with the presence of carbonaceous shales, coals, and point bar sandstones suggests a meandering river environment in the fluvio-deltaic settings (Koesoemadinata & Matasak, 1981). Furthermore, Zonneveld et al. (2012) suggest some parts of the Sawahlunto Formation was deposited within an intertidal flat setting (marginal marine setting) based on the occurrence of well-preserved avian footprints (*Aquatilavipes*) and traces attributable to the suspension feeder (*Arenicolites* and *Diplocaterion*).

1.2.4. Sawahtambang Formation

The term Sawahtambang Formation was formally proposed by Koesoemadinata & Matasak (1981) while Silitonga & Kastowo (1975) mentioned this formation as Lower Ombilin Formation in their quadrangle map. Koesoemadinata & Matasak (1981) described the Sawahtambang Formation typically consists of a thick massive sequence of light-grey to brown sandstones, mostly quartzose to feldspathic with cross-bedding sedimentary structure and the presence of conglomerates. The sandstones are poorly sorted, subangular, fine to very coarse-grained mainly conglomeratic which consist of quartz pebbles. The fining upward cycles of erosional surface, imbricated pebbles, crossbedding, and parallel lamination from the bottom to the top, respectively, become the typical sequence of the Sawahtambang Formation.

The Sawahtambang mostly exposed through the entire basin edge, from the Sigalut Plataeu, the northwest of the Ombilin Basin, and extensively in the southern area of the Ombilin Basin. Based on the field measurements by Siringo-ringo and Gunadi in Koesoemadinata & Matasak (1981), the thickness of the Sawahtambang Formation in the Sawahlunto area at least exceed up to 880 m thick. However, the data obtained from Sinamar No. 1 suggest that originally this formation is much thicker than the preserved deposits (approximately 1420 m in Sinamar No.1), evidenced by the large shift in the vitrinite reflectance and spore color index versus depth (Koning, 1985).

The relationship between the bottom unit is conformable while it is unconformably overlaid by marine sediments of the Ombilin Formation (an indication of hiatus event). Koning (1985) argued that the significant velocity difference between the Sawahtambang-Ombilin Formation yields a recognizable interface in the seismic section (Figure 15).

Palynological analysis indicates the Eocene to Oligocene in age while together with the stratigraphic correlation with the other units. Koesoemadinata & Matasak (1981) suggest the Sawahtambang Formation is presumable Oligocene in age. This formation was deposited in a fluvial dominated of supralittoral environment, presumably a braided river system through a median alluvial valley (Koesoemadinata & Matasak, 1981; Koning, 1985).

1.2.5. Ombilin Formation

The Ombilin Formation consists of a sequence of shales and marls with interbedded sandstones. The shales are generally well-laminated, dark grey in color, carbonaceous and calcareous while the marls are typically marine that contain microfossil of *globigerina*. The interbedded sandstones are typically calcareous, fine-grained, well-sorted, and contain glauconite as well as mollusks. The field measurements by Mukhayat in Koesoemadinata & Matasak (1981) show the presence of limestones nodules within marls. In the upper part, the sandstones are tuffaceous interbedded with siltstones, carbonaceous and contain glauconite and mollusks.

The distribution of the Ombilin Basin is widely located in the basin center covering almost the entire Sinamar Sub-basin. The relationship with the other units especially with the underlying Sawahtambang Formation and the overlying Ranau Formation is unconformable. This can be examined by the erosional contact at the edge of Palangki Anticline, which was revealed by the Trans Sumatra Highway construction in the past. The poorly bedded limestone can be observed on the western edge of the basin, the south of the Padangsibusuk area (Figure 11**Error! Reference source not found.**). The original thickness of the Ombilin basin is still unknown due to extensive erosion in the Late Miocene.

The presence of micro-fossils in this formation gives information about the age of the Omblin Formation. The existence of *Globigerinoides primordius* and *G. trilobus* suggests an Early Miocene in

age (N_4-N_5) (Koesoemadinata & Matasak, 1981). Together with the occurrence of glauconite and fossils determination indicate the Ombilin Formation was deposited in the outer neritic to the upper bathyal environment.

The Oil Exploration activities in the Ombilin Basin suggests that the Ombilin Formation acts as the cap rock for the Sawahtambang reservoir section (Koning, 1985).

1.3. Tertiary Volcanic

1.3.1. Ranau Formation

The volcanic identification that covers the Tertiary sediments of the Ombilin Basin is based on the characteristic correlation of rhyolitic tuff in the Bengkulu area (Barber et al., 2005). The Ranau Formation composed of mainly tuff, lava flow materials (andesite to basalt), and lahar deposits. The formation largely distributed in the North Limb of the Sinamar Sub-basin, which covers some parts of the Ombilin Basin and also a small portion near the Talawi area. The volcanic materials found within this formation is varied, from the age of Pliocene to Recent. The provenance of the Ranau Formation is predicted originated from the volcanoes on the northern area of the Ombilin Basin: Maninjau, Malintang, Merapi, and Singagalang volcanoes (Fletcher & Yarmanto, 1993). The Ranau Formation is suggested as Pliocene in age from the Late Miocene-Pliocene volcanic episode (Barber et al., 2005).